Research Square

Preprints are preliminary reports that have not undergone peer review.
They should not be considered conclusive, used to inform clinical practice,
or referenced by the media as validated information.

An escalation toward risk: climate change impacts on the distribution, genetic diversity, and conservation of Neesiochloa barbata (Poaceae: Chloridoideae: Pappophorinae)

Yuri Couceiro[1]

yuri.couceiro@ufpe.br

Universidade Federal de Pernambuco

Júlia Neves[12]

Universidade Federal de Pernambuco

Andrea Pedrosa-Harand[12]

Universidade Federal de Pernambuco

Yeison Lombo-Sanchez[1]

Universidade Federal de Pernambuco

Jefferson R. Maciel[34]

Universidade Federal Rural de Pernambuco

Cassiano A.D. Welker

Universidade Federal de Uberlândia

Marccus Alves

Universidade Federal de Pernambuco

Article

Keywords:

Posted Date: November 9th, 2026

DOI: https://doi.org/10.21203/rs.3.rs-11234385/v1

License: This work is licensed under a Creative Commons Attribution 4.0 International License.
Read Full License

Additional Declarations: No competing interests reported.

Yuri Couceiro[1]*, Júlia Neves[12], Andrea Pedrosa-Harand[12], Yeison Lombo-Sanchez[1], Jefferson R. Maciel[34], Cassiano A.D. Welker[5] & Marccus Alves[1]

[1]Programa de Pós-Graduação em Biologia Vegetal, Universidade Federal de Pernambuco, Recife, PE, Brazil

[2]Laboratório de Citogenética e Evolução Vegetal, Departamento de Botânica, Centro de Biociências, Universidade Federal de Pernambuco, Recife -PE, 50670-901, Brazil

[3]Prefeitura da Cidade do Recife, Jardim Botânico do Recife, Recife, PE, Brazil

[4]Programa de Pós-Graduação em Biodiversidade, Universidade Federal Rural de Pernambuco, Recife, PE, Brazil

[5]Programa de Pós-Graduação em Biologia Vegetal, Universidade Federal de Uberlândia, Uberlândia, MG, Brazil

Corresponding author: yuri.couceiro@ufpe.br

An escalation toward risk: climate change impacts on the distribution, genetic diversity, and conservation of *Neesiochloa barbata* (Poaceae: Chloridoideae: Pappophorinae)

***short running title**: climate change impacts in Neesiochloa barbata*

Abstract

Climate change represents a primary threat to global biodiversity, particularly in seasonally dry tropical forests (SDTF), affecting species distribution, genetic diversity, and ecosystem conservation. *Neesiochloa barbata* (Poaceae: Chloridoideae: Pappophorinae) is a grass species belonging to a monotypic genus endemic to the Caatinga, the largest SDTF in South America. In this study, we addressed conservation issues related to the impacts of the climate crisis (2080–2100) on the potential distribution, genetic diversity, and structure of *N. barbata* populations to: (a) assess extinction risk; (b) estimate the future distribution overlap with protected areas (PA); and (c) identify priority areas for conservation. We assessed the current conservation status from Not Evaluated (NE) to Least Concern (LC), however, under future climate scenarios, suitable habitat for *N. barbata* will be reduced, elevating the threat level to Near Threatened (NT) and finally to Endangered (EN). This severe contraction of climatically suitable areas results in a progressive escalation in extinction risk: LC > NT > EN. Despite the overall loss of suitable habitat, the remaining future niche shows a slight spatial shift toward the boundaries of existing PA (increasing from 39% to 43%). The haplotype network (nrDNA and cpDNA) showed distinct polymorphism rates between the genomes, consistent with the DAPC clustering (best K = 2 and Northern and Southern haplogroups). This genetic structure highlights lineages with distinct evolutionary histories that must be preserved. The reduction in suitable areas and the rising extinction risk underscore the urgent need for targeted conservation in the Caatinga. While the current PA system is crucial for protecting climatic refugia, the expansion and connection of these areas are essential to ensure the long-term persistence and genetic heritage of *N. barbata* against the climate crisis.

Keywords – Caatinga, genome resequencing, heterozygosity, IUCN, Neotropics, SSP

Introduction

The exponential increase in global temperature is one of the main threats to biodiversity, particularly to seasonally dry tropical forests (SDTF) [1-2], especially in the Americas [3]. Climate change associated with anthropogenic factors has driven declines in diversity across distinct biological groups in the Neotropical region, a globally recognized biodiversity hotspot [4]. This climatic scenario is expected to intensify in the short term [5-6].

The Caatinga, one of the largest SDTFs in the South America and exclusive to Brazil (total area extension of the Caatinga is ~833,000 km², [7-8], faces comparable threats across a wide range of environmental and climatic gradients [9,7], in addition to anthropogenic pressures [10-11] and desertification processes [12]. This phytogeographic domain extends beyond northern Minas Gerais state and covers a broad area of northeastern Brazil, comprising distinct vegetation types and edaphic formations [13] under a semi-arid tropical climate with low precipitation (< 300–1,000 mm year) [14]. Its origin dates back to the Miocene, harboring tens of millions of years of evolutionary history of several lineages that specialized in arid and semi-arid regions of the Americas (e.g., dry forests and savannas) [15].

In the Brazilian flora, there are approximately 18.783 endemic flowering plant species [16], of which 526 (2.8%, [8]) to 1149 (6.1%, [17]) are restricted to the Caatinga. Endemic species can be accurate and independent predictors of organismal responses to climate change [18], even at broad spatial scales [19]. Given the environmental filter imposed by the remarkable conditions of the Caatinga (high temperatures and low precipitation), populations of species that collapse seasonally (e.g., annual species) and are exposed to intense anthropogenic pressures are particularly sensitive to climate change [20]. Ecological niche models (ENM) have been widely used to project and estimate the effects of the climate crisis on species distributions [21-22]. Both contractions of climatically suitable areas [23] and potential expansions of geographic ranges have been reported for angiosperms [24-25], including several grass lineages [26-27].

In addition to climatic modeling approaches, low-coverage whole-genome sequencing (lcWGS) represents a cost-effective and highly informative tool for population genomic studies under climate change scenarios [28]. Key questions for biodiversity conservation, such as population delimitation and the assessment of genetic structure and connectivity, can be addressed using genomic tools [29]. Over the past two decades, several whole-genome assemblies in Poaceae (e.g. rice and maize, [30-31]) have been generated and can serve as references also for conservation-oriented studies. Although challenging, investigating the genetic diversity of endemic lineages from SDTF is particularly valuable for the maintenance

of local genetic heritage [32], as well as for identifying areas of high biological relevance and priority for conservation [33]. The Caatinga may harbor endemic lineages with high levels of local adaptation [18], and the identification of single nucleotide polymorphism (SNP) markers is especially useful for conservation genomics [34-35]. Therefore, failure to conserve endemic lineages contributes to the erosion of the global genetic heritage, particularly in a context in which initiatives focused on Caatinga grasses remain poorly explored.

Neesiochloa barbata (Nees) Pilg. (Poaceae: Chloridoideae: Pappophorinae) is a grass species belonging to a monotypic genus and is endemic to the Caatinga SDTF, with known populations restricted to small and localized areas [36]. Diagnostic traits (Figure 1) of this species include its annual life cycle (i.e., populations collapse during the life cycle), small stature (< 40 cm length), lax inflorescences, and long pedicels bearing awned spikelets with 7–10 florets arranged in a fan-like pattern [37]. Little is known about its potential threats and conservation status (Not Evaluated – NE [38]). Examining the effects of climate change on patterns of distribution, genetic diversity, and population structure of endemic species can support strategies to mitigate the decline of natural populations in the Caatinga [18].

To address conservation questions related to the impacts of the climate crisis on the potential geographic distribution and genetic diversity and structure of *Neesiochloa barbata* in the Caatinga, we evaluated how different climate scenarios (optimistic and pessimistic) may affect the future availability of climatically suitable areas for the species. We also examined the genetic diversity of natural populations in order to (a) estimate extinction risk, (b) quantify how much of the future distribution will overlap with protected areas (PA), and (c) identify priority areas for conservation within the Caatinga SDTF.

Materials and Methods

Plant material

We conducted field expeditions in northeastern Brazil between April and August 2024, covering the states of Bahia, Paraíba, Pernambuco, and Rio Grande do Norte (Figure 2). We visually estimated the number of individuals per population using a 100-m linear transect and selected the most spatially distant individuals within each population for molecular sampling (Table 1). The *Neesiochloa barbata* specimens were identified by Yuri Couceiro, Cassiano A. D. Welker and Jefferson Maciel. We collected leaf fragments from five populations (six samples per population) and preserved the tissue in silica gel to maintain genomic DNA integrity. Finally, we deposited voucher specimens representing each population in the UFP Herbarium ([39]acronym continuously updated). All research and fieldwork involving wild plant material complied with relevant institutional, national, and international guidelines and

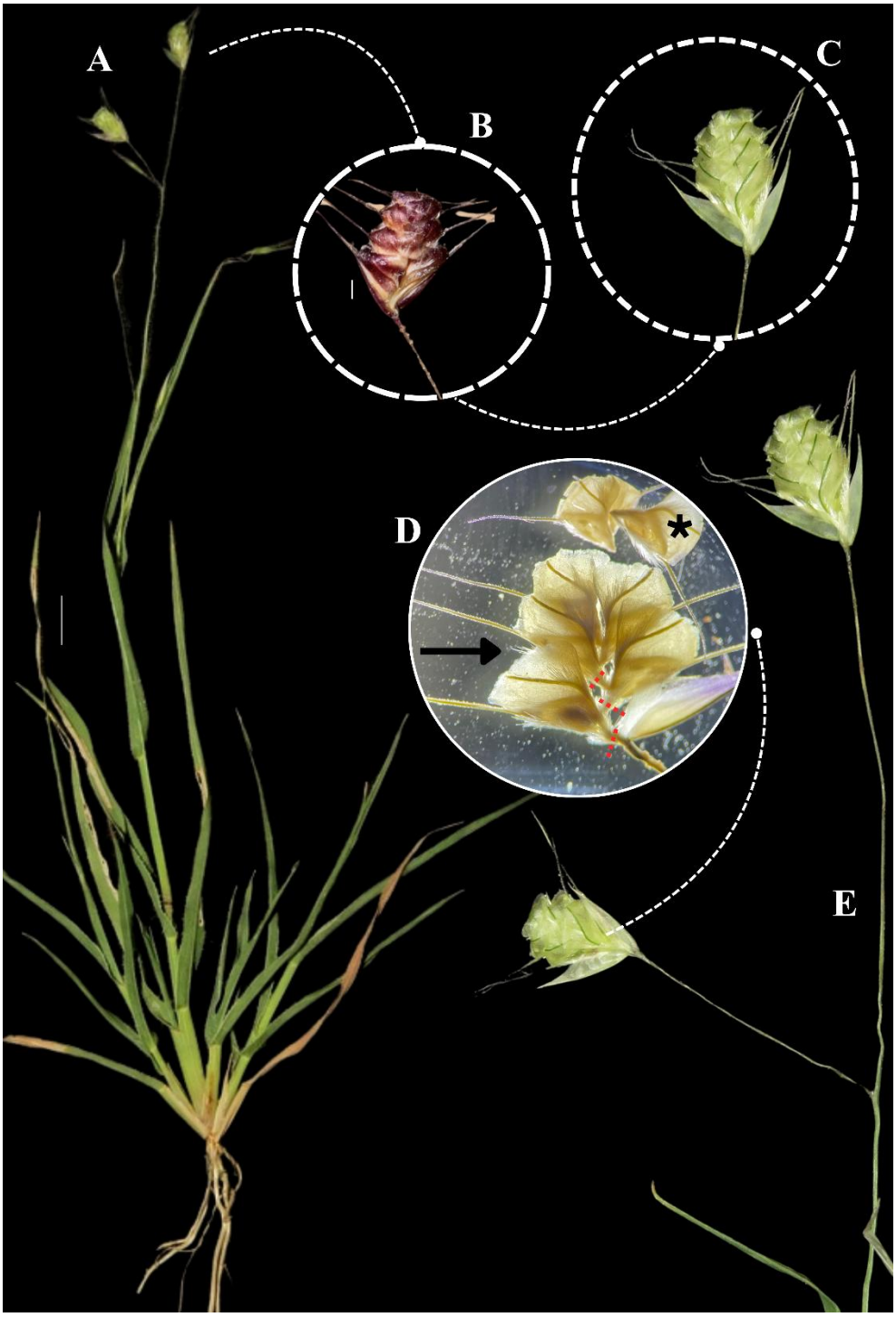
117 legislation. The study was conducted in accordance with the IUCN Policy Statement on
118 Research Involving Species at Risk of Extinction and with the Convention on International
119 Trade in Endangered Species of Wild Fauna and Flora (CITES), where applicable.

120 **Table 1.** Population codes, localities in Brazil, estimated sizes, and herbarium vouchers for the
121 *Neesiochloa barbata* samples. Estimated size represents individuals visually estimated along a
122 100-m transect. RN = Rio Grande do Norte state; PE = Pernambuco state; PB = Paraíba state.

Population code	Population locality	Estimated size	Herbarium voucher
MU	Sítio Mulungu, Salgueiro, PE	≤ 200	*Couceiro 751* (UFP 101769)
PF	Pau Ferro, Salgueiro, PE	≤ 150	*Couceiro 750* (UFP 101768)
SP	Selva de Pedras, Patos, PB	≤ 100	*Couceiro 752* (UFP 101770)
CA	Carnaúbinhas village, Serra Negra do Norte, RN	≤ 100	*Couceiro 753* (UFP 101771)
TB	Timbaúba dos Batistas, RN	≤ 50	*Couceiro 754* (UFP 101757)

123

124 **Figure 1.** Morphological traits of *Neesiochloa barbata*. **A)** Plant habit: general view of the
125 entire plant, highlighting the basal branching system and the inflorescence; scale bar = 1 cm.
126 **(B)** Detail of vinaceous (young) and **(C)** stramineous (mature) spikelets; scale bar = 1 mm. **(D)**
127 Detail of awned florets and caryopsis organization within the spikelet: the black arrow indicates
128 florets still attached to the rachilla, the asterisk marks detached florets ready for dispersal
129 (diaspores), and red dashed lines indicate the disarticulation zones between florets. **(E)** portion
130 of branch in the inflorescence. Photo credit: José Vinícius and Yuri Couceiro (Available under
131 Creative Commons CC-BY 4.0 license).

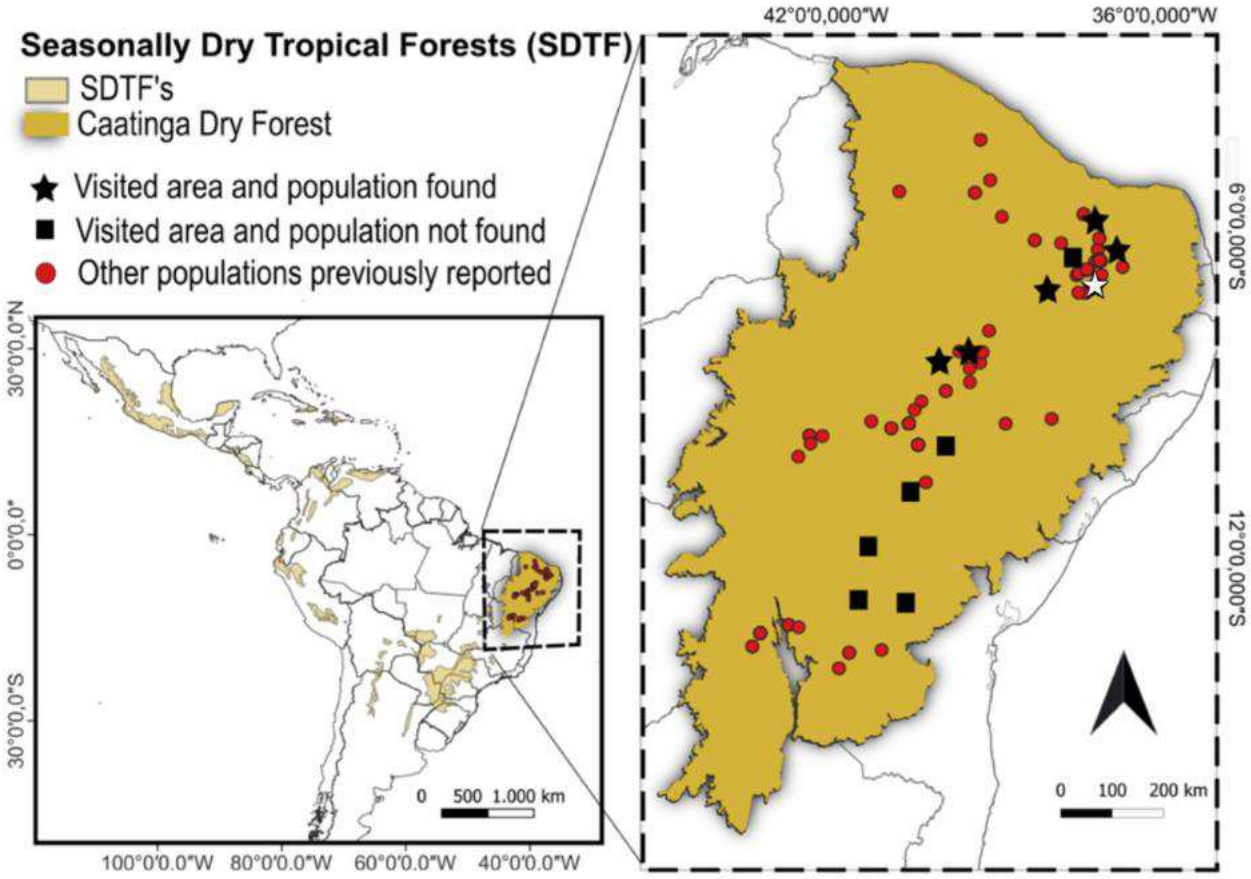


Georeferenced data

We built a data matrix using geographic distribution records of *Neesiochloa barbata* obtained from the Global Biodiversity Information Facility (GBIF [40]), Reflora – Herbário Virtual [41], and SpeciesLink [42]. The following collections, including type material (*), were also consulted: ALCB, ASE, CEN, CEPEC, EAC, HEPH, HRSN, HUEFS*, HUFU, HVASF, IBGE, IPA*, JPB, MAC, MOSS, PEUFR, RN, UB, UFP, and UFRN ([39] acronyms continuously updated). The species' known distribution remains restricted to the Caatinga

SDTF, where we found populations in typical landscape shrub–herbaceous vegetation, with relatively homogeneous density, on stony–sandy soils (Figure S1).

Figure 2. Known geographic distribution of *Neesiochloa barbata* in Caatinga SDTF. The detailed map (right) contrasts historical occurrence records (red circles) with the current field expeditions (stars and squares). The map symbols are intentionally scaled out of proportion to emphasize the sampling effort across these areas. The white star represents a single collected individual (*Couceiro 174*, UFP98098), which provided an insufficient sample size for genetic analysis.



Environmental variables

We obtained 19 bioclimatic variables from WorldClim v. 2.1 at a 2.5 arcminutes resolution [43]. To reduce multicollinearity, we calculated pairwise Pearson correlation coefficients from current climate data and excluded variables with $|r| \geq 0.70$ [44]. We retained five variables: bio_3 (isothermality), bio_12 (annual precipitation), bio_14 (precipitation of the driest month), bio_18 (precipitation of the warmest quarter), and bio_19 (precipitation of the coldest quarter) (Table S1).

Environmental suitability modeling and projection

We modeled the potential distribution of *Neesiochloa barbata* using the '*modleR*' package in R v.4.4.0 [45] and applied cross-validation techniques to assess model robustness [46]. We configured occurrence data using the '*setup_sdmdata*' function and employed

multiple algorithms to estimate potential distribution: Maximum Entropy (MaxEnt [47]), Generalized Linear Models (GLM [48]), Support Vector Machines (SVM [49-50]), Random Forest [51], and Boosted Regression Trees (BRT [52]). We used the '*do_many_function*' to run these algorithms and the '*final_model*' function to produce a consensus model. We evaluated model performance using the area under the receiver operating characteristic (ROC) curve (AUC).

To generate future climate projections (2080–2100), we selected three General Circulation Models (GCMs): CNRM (a physical climate model with atmosphere–ocean coupling and detailed atmospheric and land-surface parameterizations), MIROC6 (a physical climate model with coupled atmosphere–ocean dynamics and advanced representation of large-scale circulation processes), and MRI-ESM2-0 (an Earth system model that, in addition to physical climate processes, explicitly represents biogeochemical cycles and atmospheric composition). We projected scenarios based on two Shared Socioeconomic Pathways (SSP; standardized socio-economic and land-use trajectories used to drive climate simulations): SSP2-4.5 (an intermediate greenhouse-gas emissions scenario = optimistic) and SSP5-8.5 (a high-emissions scenario = pessimistic). We defined the projection area within the Caatinga SDTF boundaries plus a 1.5° buffer.

To quantify suitability, we converted continuous maps into binary maps (presence/absence) by applying a threshold that maximizes the True Skill Statistic (TSS). We chose the threshold to ensure an optimal balance between sensitivity and specificity, providing a robust trade-off between identifying known occurrences and minimizing overprediction [53-54]. We calculated the total suitable area using the *'expanse'* function from the terra package [55]. Finally, we estimated the percentage of suitable areas covered by protected areas (PA) using the mask '*thr projs mscn b*' function from the ENMwizard package [56-57], identifying PA through the World Database on Protected Areas (WDPA; [58]). All analyses were performed in R v.4.4.0 [45]. We finally classified any land area within the Caatinga SDTF domain with some level of conservation defined as a PA. Only 9% (~ 76,000 km²) of the Caatinga has some level of protection [59], and of that, only 2% (~ 16,889 km²) concentrate the units with the most restrictive limits to human intervention (such as different conservation categories).

Extinction risk based on potential and projected species distribution

We assessed extinction risk by estimating projected changes in area of occupancy (AOO) following IUCN Red List criteria [60]. We adapted Criterion A3(c) to quantify the

proportional reduction in suitable habitat between current and future projections [61-[62]. Extinction risk categories were assigned independently for each scenario (SSP2-4.5 and SSP5-8.5) based on the magnitude of habitat loss as follows: Extinct (EX): 100% loss of suitable habitat, Critically Endangered (CR): loss of > 80% of suitable habitat, Endangered (EN): Loss of 50–80% of suitable habitat. Vulnerable (VU): loss of 30–50% of suitable habitat, Near Threatened (NT): loss of < 30% of suitable habitat and Least Concern (LC): no projected loss of suitable habitat. For the current status, we considered the modeled extent of suitable habitat (AOO): CR: < 100 km², EN: < 5,000 km², VU: < 20,000 km², NT: < 30,000 km² and LC: > 30,000 km² [60].

DNA extraction and sequencing

We extracted total genomic DNA from young tissues using the CTAB (cetyl-trimethylammonium bromide) protocol [63]. We assessed DNA integrity on 1% (w/v) agarose gels and quantified samples using a NanoDrop spectrophotometer to standardize concentrations. We sequenced the DNA using the DNBseq approach (BGI), generating 150-bp reads and at least 1 Gb of data per individual.

Genetic diversity and population structure analyses

We mapped raw reads against reference sequences using Geneious software v. 9.1.8, the *Bouteloua curtipendula* (Michx.) Torr. (NCBI accession NC_029414.1) plastome and the *Sporobolus maritimus* (Curtis) P. M. Peterson & Saarela (NCBI accession GCA_965119375.1) nuclear 35S nrDNA cistron. After mapping, we aligned sequences using MAFFT [64]. Following the methodology of Mäder et al. [65], we generated haplotype networks for both genomes using the median-joining (ε = 0; [66]) approach implemented in PopArt v.1.7 (Population Analysis with Reticulate Trees; [67]. All newly generated genome sequences will be available in the National Center for Biotechnology Information (NCBI) database.

We estimated genetic diversity and performed an Analysis of Molecular Variance (AMOVA; [68] with 10,000 permutations in Arlequin [69]. We assessed population structure via Principal Component Analysis (PCA) and genetic clustering in the adegenet package [70]. We determined the optimal number of clusters (best K) using the Bayesian Information Criterion (BIC) and performed a Discriminant Analysis of Principal Components (DAPC). We generated all graphical outputs in R, using '*scatter.dapc*' for spatial clustering and '*barplot*' for membership probabilities. Graphical outputs were generated using the '*scatter.dapc*' function for spatial clustering and the R base '*barplot*' function for membership probability visualization, with data organization handled by the '*order*' and '*transpose*' functions to align genetic results with sampling metadata [45].

Phylogenetic reconstructions and divergence time estimations were performed using Bayesian Inference in BEAST v1.8.4 [71]. The dataset comprised sequences from the nuclear ribosomal internal transcribed spacer (ITS) and five plastid regions (*rps16-trnK*, *rps16*-intron, *rpl32-trnL, ndhF*, and *ndhA*-intron) obtained from the 17 species of the subtribe Pappophorinae (Table S2).

For both genomic matrix (cpDNA and nrDNA), an uncorrelated relaxed molecular clock model with rates drawn from a log-normal distribution was implemented, associated with the Yule speciation process [72-73] as the tree prior. Markov Chain Monte Carlo (MCMC) simulations were run for 10^8 generations, sampling every 10^4 iterations. Parameter convergence and sampling adequacy (Effective Sample Size, ESS > 200) were confirmed using Tracer v1.7.2 [74], after discarding the initial 10% of the trees as burn-in. However, due to low node support and unresolved polytomies in our Bayesian inference (BI), we additionally employed a Maximum Likelihood (ML) approach. We constructed ML trees using FastTree v2.1.11 [75].

Temporal calibration was based on a secondary calibration point from [76]. To account for statistical uncertainty, a normal distribution was applied to the node corresponding to the tribe Pappophorinae, with a mean of 18.02 Ma and a standard deviation of 1.09 (adjusted to encompass the 10% confidence interval reported in the reference study).

Results

Climate modeling for Neesiochloa barbata

Under current climatic conditions, *Neesiochloa barbata* exhibits a broad potential distribution, as estimated by ecological niche models, within the Caatinga SDTF domain. Areas of higher suitability and range are concentrated mainly in the central and northern portions of the Caatinga SDTF (Figure 3A). The total environmentally suitable area is approximately 233,672.4 km², indicating that current climatic conditions are favorable across a large portion of the species' potential range, although not uniformly across the entire domain. In contrast, future projections indicate a drastic contraction of climatically suitable areas (Figures 3B–C, S2). Under the optimistic scenario (SSP2–4.5), the suitable area is reduced to 167,990.7 km², representing a loss of 28.11 %. Under the pessimistic scenario (SSP5–8.5), it decreases further to 110,108.6 km², representing a severe habitat reduction of 52.88%.

Despite this continuous reduction in the total environmentally suitable area, the proportion of this habitat located within PA increases slightly, from 39.14% under current conditions to 39.51% (SSP2–4.5) and 43.63% (SSP5–8.5). This pattern reflects a spatial contraction where the remaining suitable areas are increasingly concentrated in regions that overlap with existing protected areas (PA), rather than an absolute increase in protection

coverage. In fact, the absolute protected suitable area shrinks from 91,467.15 km² (current scenario) to 48,035.09 km² (SSP5-8.5 scenario) (Table 2).

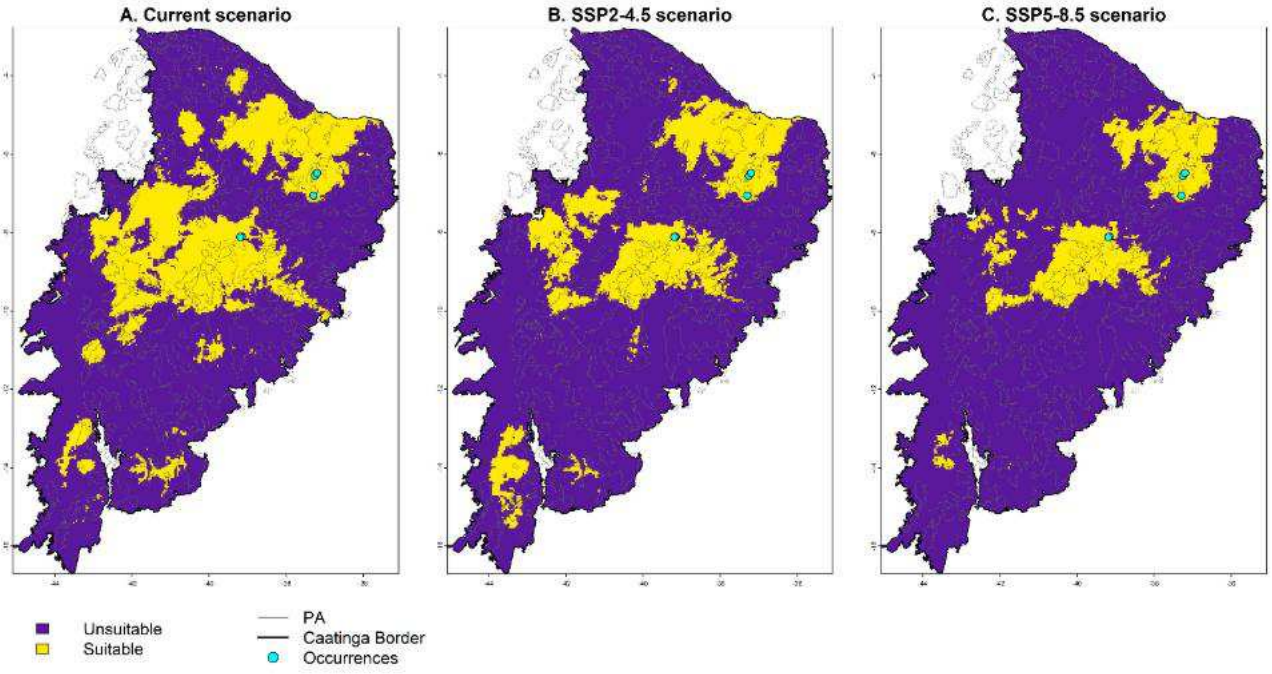
Table 2. Environmental suitability area (km²), extension and percentage of suitable area within protected areas (PA), Area of Occupancy (AOO; km²), and extinction risk category based on IUCN Criterion A3(c) for *Neesiochloa barbata*. under current and future climate scenarios. Environmental suitability area and protected area coverage were derived from species distribution models, whereas AOO was used exclusively to assess extinction risk and was calculated independently.

Climatic scenario	Suitability area (km²)	PA (km²)	PA (%)	AOO (km²)	Criterion A3(c)
current	233,672.4	91,467.15	39.14	44,192	**LC**
optmistic (SSP2–4.5)	167,990.7	66,365.43	39.51	31,780	**NT**
pessimistic (SSP5–8.5)	110,108.6	48,035.09	43.63	20,800	**EN**

The risk of extinction was assessed using both the projected loss of suitable habitat and changes in projected area of occupancy (AOO). Under current conditions, the species is classified as Least Concern (LC), with an AOO of 44,192 km² (Table 2). However, in future scenarios, the AOO is projected to decrease to 31,780 km² (SSP2–4.5) and 20,800 km² (SSP5–8.5). Consequently, based on the projected proportional reduction of suitable habitat (Criterion A3c), the extinction risk for *N. barbata* increases to Near Threatened (NT) in the optimistic scenario (SSP2–4.5) and intensifies further to Endangered (EN) in the pessimistic scenario (SSP5–8.5), evidencing a substantial escalation in its vulnerability to climate change.

Figure 3. Binary potential distribution of *Neesiochloa barbata* under different climate scenarios. **(A)** Current scenario; (**B)** Optimistic scenario (SSP2-4.5) and (**C)** Pessimistic scenario (SSP5-8.5). Suitable areas (yellow) and unsuitable areas (purple) were derived from species distribution models using a threshold (< 70% suitable) that maximizes the True Skill Statistic (TSS). Green circles indicate the sampling localities of the populations subjected to genetic analyses (MU, PF, SP, CA, and TB). The solid-line outlines represent the boundaries

of protected areas (PA) in the Caatinga SDTF.



Genetic diversity and population structure of natural populations of Neesiochloa barbata

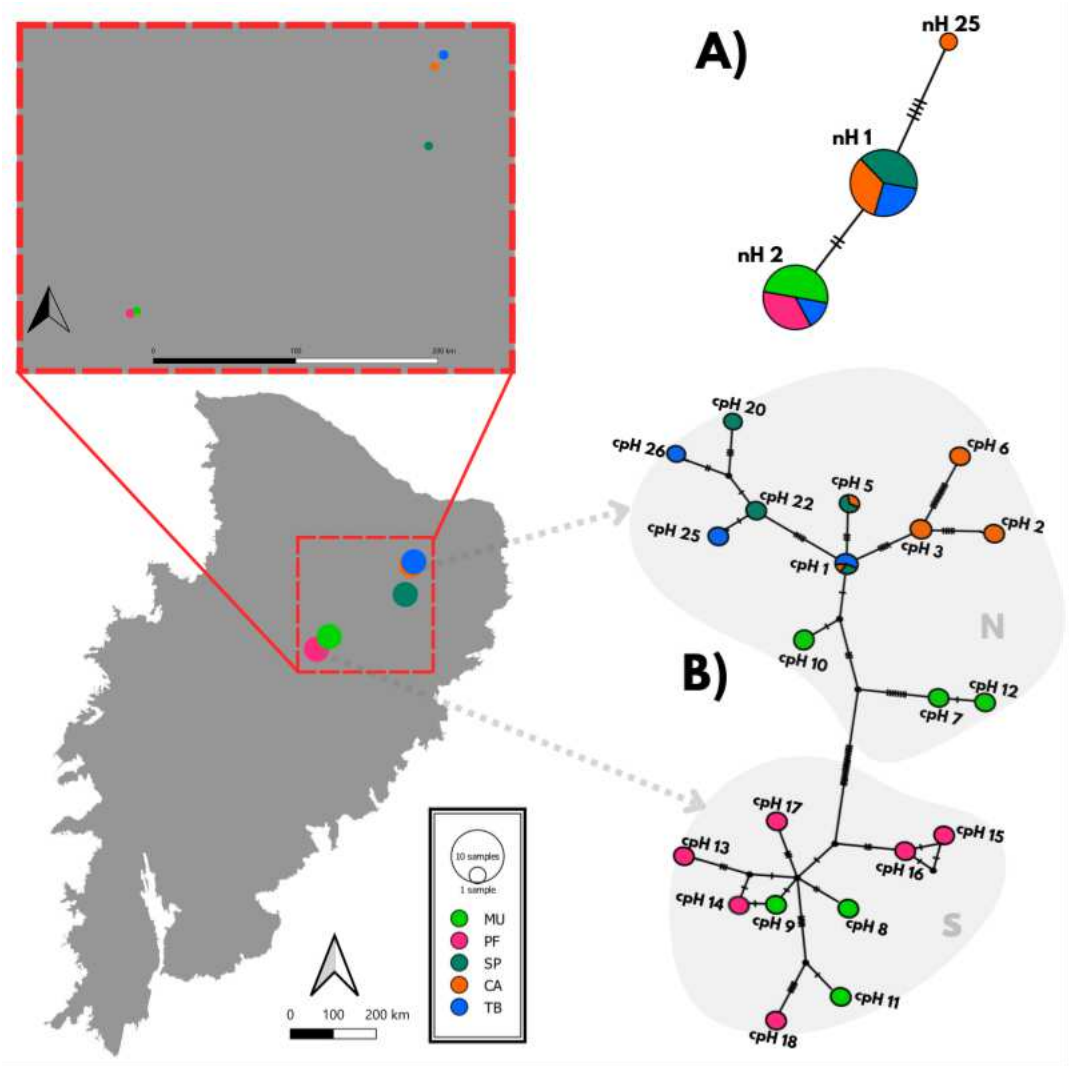
The nuclear (nrDNA) sequences showed weaker geographic structure, higher genetic similarity among individuals, and consequently lower haplotypic diversity (Figure 4A). Only three haplotypes were detected in the nrDNA network (nH 1, nH 2, and nH 25). Haplotype nH 1 comprised individuals from the three northern populations (SP, CA, and TB); nH 2 grouped the southern populations together with some individuals from TB, and nH 25 was represented exclusively by individual CA06 from a northern population. This individual was highly divergent from the remaining CA individuals grouped in nH1, being separated by several mutational steps.

After inspection of the BIC plots, two genetic clusters were inferred for the nrDNA (K = 2) and two clusters for the cpDNA dataset (K = 2) (Figure 5). The north–south structure was recovered in the nrDNA dataset, though with increased admixture in population TB (Figure 5A, blue bars) that shows evidence of gene flow between the N and S distribution ranges. Specifically, individuals TB02 and TB05 function as a genetic bridge, sharing profiles with the southern populations (MU and PF). While the southern populations remain consistent in nrDNA (Figure 5A, blue bars), they exhibit northward mixing with TB. This occurs conversely in cpDNA northern genetic signatures (Figure 5B, red bars) intermingle with southern individuals (red bars, MU01, MU03, and MU06). This suggests that the genetic signatures at the geographical extremes: TB in the north (nrDNA) and MU in the south (cpDNA).

In contrast, plastid (cpDNA) haplotype network revealed two major groups (haplogroups) showing a clear north–south geographic structure among populations (Figure 4B). Haplogroup N predominantly comprised the northern populations, namely SP, CA, and TB. Some haplotypes were shared among populations, with haplotype cpH 1 shared by all three northern populations and haplotype cpH 5 shared only between CA and SP. Haplogroup S, separated from haplogroup N by several mutational steps, comprised the southern populations MU and PF. Within haplogroup S, each individual displayed a unique haplotype separated by multiple mutational steps, indicating higher haplotypic diversity than that observed in haplogroup N. In addition, eight putative median vectors were inferred (Figure 4B, black points), which were necessary to resolve the evolutionary relationships among individuals. Notably, some individuals from the MU population were placed within haplogroup N (cpH 7, cpH 10 and cpH 12), despite MU being geographically located in the southern portion of the sampling area. MU population acts as a bridge between the two genetic groups, connecting northern and southern populations.

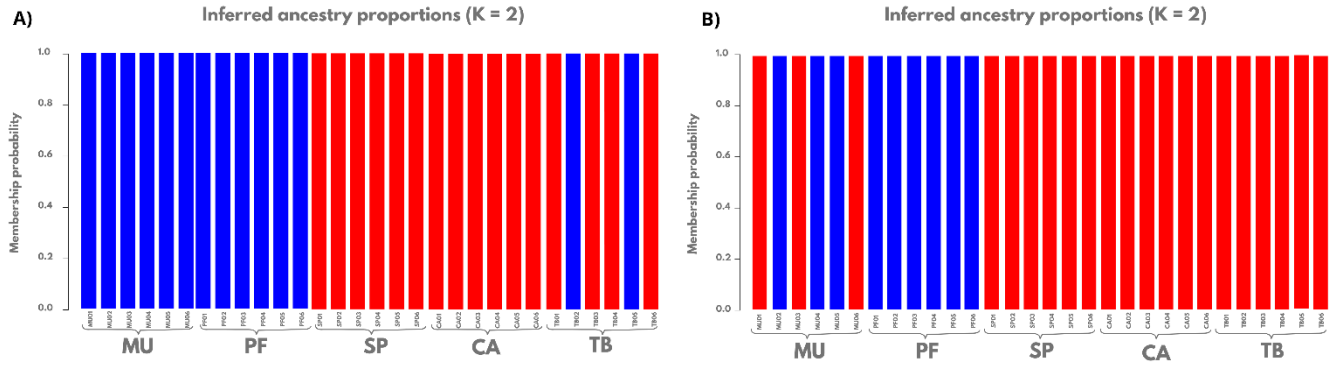
The two-cluster structure recovered for the plastome (cpDNA) is consistent with the north–south pattern observed in the haplotype network (Figure 5B; haplogroup N and S). Accordingly, the three northern populations (SP, CA, and TB) are composed of individuals genetically attributed to the first cluster (Figure 5B, red bars). Evidence of interpopulation gene flow is indicated within MU population (MU01, MU03, and MU06) which displays a genetic profile typical of SP, CA, and TB, whose genetic composition is like that of the north populations. The southern populations (MU and PF) show similar genetic compositions (blue bars), but only individuals MU02, MU04 and, MU05 represented the admixture, southern cluster. The MU individuals showed admixture clusters N and S.

Figure 4. Geographic distribution and phylogeographic structure of *Neesiochloa barbata* populations. The map illustrates the sampling localities within the Brazilian Northeast, with a detailed inset of the collection sites. **(A)** Nuclear nrDNA haplotype network (nH) showing low divergence and shared ancestral alleles among populations. **(B)** Plastid cpDNA haplotype network (cpH) exhibiting high structured diversity. Haplogroups are highlighted by shaded areas, indicating a genetic split between the Northern **(N)** and Southern **(S)** regions. Colors correspond to the following populations: **MU** (Sítio Mulungu, PE – light green); **PF** (Pau Ferro, PE – pink); **SP** (Selva de Pedras, PB – dark green); **CA** (Carnaúbinhas, RN – orange), and **TB** (Timbaúba dos Batistas, RN – blue). Circle sizes are proportional to haplotype frequency, and black bars **(-)** on branches represent the number of mutational steps.



338

339 **Figure 5.** Genetic assignment and population structure of *Neesiochloa barbata* based on
340 Bayesian clustering. Bar plots represent the inferred ancestry proportions for 30 individuals
341 across five populations for **(A)** nrDNA and **(B)** cpDNA cluster, both optimized at K = 2.
342 Clusters are shown in red and blue bars. Populations are delimited from each other by brackets,
343 corresponding to their geographic localities: MU (Sítio Mulungu, PE), PF (Pau Ferro, PE), SP
344 (Selva de Pedras, PB), CA (Carnaúbinhas, RN), and TB (Timbaúba dos Batistas, RN). The
345 vertical bars indicate individual membership probabilities, highlighting a clear genetic split
346 between northern (SP, CA, TB) and southern (MU, PF) populations.



Molecular diversity indices were lower for the nrDNA than for the cpDNA dataset (Table 3). The mean expected heterozygosity (H_e) for the nrDNA was 0.08, with the highest value observed in TB (0.26), whereas the mean for plastome was 0.19, with the CA population showing the highest values (0.24, Table 3). In this sense, the mean plastid H_e indicates that, although this genome is generally considered less variable, a measurable level of within-population genetic diversity is maintained (60.41%, Table 4). For nrDNA, the low heterozygosity values in most populations align with the reduced SNPs (single nucleotide polymorphism) diversity in the haplotype network, indicating high levels of nrDNA repeat homogenization across populations.

AMOVA results corroborated moderate to high levels of genetic differentiation among populations, with F_{st} values of 0.74 for nrDNA and 0.39 for the cpDNA (Table 4). These results demonstrate significant population structure, consistent with the spatial division into two distinct genetic lineages (northern and southern groups) identified in the phylogenetic and network analyses.

Table 3. Summary of molecular diversity indices (expected heterozygosity – H_e) for the nuclear (nrDNA) and plastid (cpDNA) gene compartments in the sampled populations of *Neesiochloa barbata*.

Populations	H_e (nrDNA)	H_e (cpDNA)
MU	0.00	0.17
PF	0.00	0.18
SP	0.00	0.17
CA	0.16	0.24
TB	0.26	0.17
Mean	0.08	0.19

Table 4. Molecular analysis of variance (AMOVA) for the nuclear (nrDNA) and plastid (cpDNA) markers, indicating the partitioning of genetic variation within and among populations and the respective fixation index (F_{st}) values.

Variation source	nrDNA (%)	cpDNA (%)
Among populations	74.00	39.59
Within populations	26.00	60.41
F_{st}	0.74	0.39

Phylogenetic topology and lineages recovered

The ML tree based on cpDNA sequences recovered *Neesiochloa barbata* as a monophyletic lineage that diverged during the Miocene (~12.8 Ma, SH-like support = 1.0). The internal topology of the species reveals a branching event at approximately 9.6 Ma (SH-like support = 0.99), which segregated a clade predominantly composed of individuals from the southern Mulungu site (MU01, MU02, MU04) and Pau Ferro (PF02) from the other lineages. Although none of the five sampled populations were recovered as an intraspecific monophyletic group, the subsequent topology exhibits strong radiation (Figure S3). Terminal lineages did not cluster by geographic origin; instead, individuals from different localities appeared widely intermixed across the clades (Figure 6). Phylogenetic reconstruction based on the plastome (cpDNA) dataset using Bayesian inference resulted in a poorly resolved topology.

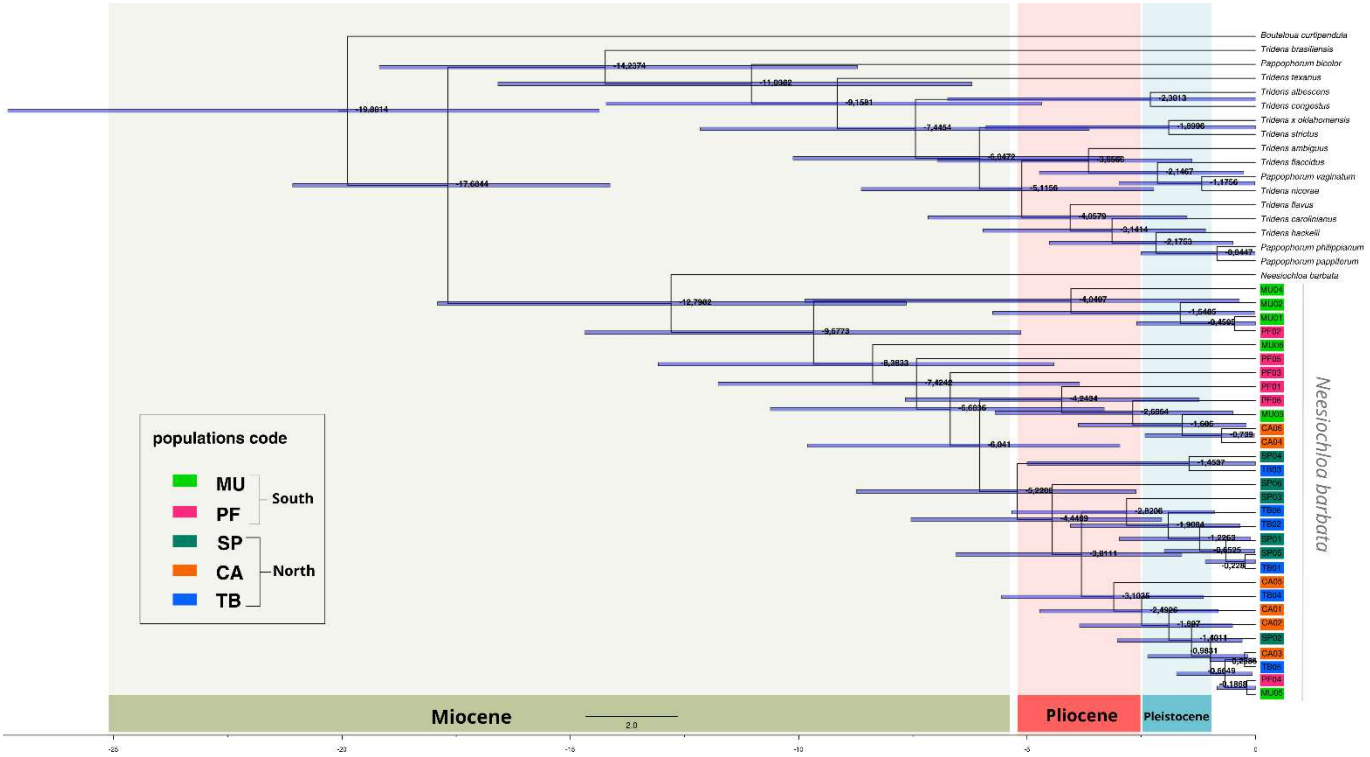
Northern localities (CA, TB, SP) do not form exclusive and population-specific clades. Instead, they emerge as independent terminal branches or small pairs of sister lineages (e.g., SP06–SP03 and TB06–TB02) that are generally embedded within a larger clade of admixed lineages. In the southern localities (MU, PF), they are highly polyphyletic in almost all major subclades of the tree. An example is MU05 and PF04, which form a highly derived terminal pair and diverged recently (~0.18 Ma), while other MU and PF individuals occupy deeper branching positions closer to the root of the radiation.

Phylogenetic reconstruction based on the nuclear (nrDNA) dataset using Bayesian inference resulted in a poorly resolved topology characterized by extremely low node support and extensive polytomies (Figure S4). The low polymorphism observed in the nrDNA may explain the low resolution of the nodes. To overcome this lack of internal resolution, a maximum-likelihood approach was employed via FastTree (Figure S5).

Southern populations (MU and PF), along with two northern individuals (TB02 and TB05), collapsed into a polytomy (Figure S4). Conversely, a divergent lineage grouped the remaining northern populations (CA, SP, and individuals TB01, TB03, and TB04), with CA06 emerging as the most basal branch (sister to the rest of the individuals in this subclade; support value = 0.8).

Figure 6. Maximum Likelihood phylogenetic tree showing divergence times estimated via Bayesian inference implemented in BEAST. The time-calibrated phylogeny of *Neesiochloa barbata* populations and other Pappophorinae taxa was based on plastid sequences (cpDNA). Node values represent mean divergence times in millions of years (Ma), and blue horizontal bars indicate 95% uncertainty intervals highest posterior density (HPD) for node ages. Colored squares at the terminals correspond to the five sampled populations (MU, PF, SP, CA, and TB), sequenced via low-coverage whole-genome sequencing (lcWGS). The named species in terminal indicates access composed of plastid gene sequences (*rps16-trnK*, *rps16-intron*,

rpl32-trnL, ndhF, and *ndhA-intron*) retrieved from GenBank. Scale bar = 2.0 Ma.



Discussion

Environmental changes drive global shifts in species distributions, threatening biodiversity persistence by restricting climatically suitable habitats and altering evolutionary trajectories. Evaluating these impacts is critical for endemic taxa in vulnerable ecosystems (such as Caatinga), where survival often depends on local climate refugia and adaptive capacity. In this study, we tested how future climate scenarios will affect the distribution and genetic integrity of *Neesiochloa barbata*, an endemic grass of the Caatinga SDTF. Our key findings reveal a drastic projected range contraction elevated to Endangered (EN) status under pessimistic scenarios, alongside strong genetic structuring that highlights peripheral populations as critical targets for conservation.

Our results indicate that, although rising temperatures drive a strong retraction in suitable areas, populations of *Neesiochloa barbata* are projected to persist in climatic refugia until the end of the century (2081–2100). Projections suggest substantial shifts in the climatic structure of the Caatinga, especially regarding annual precipitation (bio_12) and precipitation of the coldest quarter (bio_19), which exhibited the highest fluctuations across scenarios. Precipitation acts as a selective force that can drive local adaptation in grasses; in *Andropogon gerardi* Vitman (Poaceae: Panicoideae), for instance, rainfall gradients shape gene expression and cause variations in the phenotype, resulting in maximum fitness within home environments [77]. A similar bioclimatic dependence is reflected in *N. barbata* across over two centuries of sampling efforts (e.g., SpeciesLink), which reveal an increase in records between February and May (1817–2026). Because this period coincides with rainfall exceeding 200 mm in the Caatinga SDTF [13], our findings suggest that the phenological and evolutionary dynamics of *N. barbata* may be regulated by annual precipitation variance.

The IUCN [78] recommends re-assessments every five years; however, many species still lack an initial conservation assessment. To date, efforts to properly evaluate and classify the conservation status of *Neesiochloa barbata* have been unprecedented (NE: Not Evaluated), and we expect the results presented here to support future conservation actions in the Caatinga SDTF. We currently classify the extinction risk of *N. barbata* as Least Concern (LC), based on its current area of occupancy (AOO = 44,192 km²). The broad suitability projected for the Caatinga indicates that current climatic conditions are favorable for the species across much of the domain, even if it only partially occupies the available climatic space. However, taxa occurring in SDTF, especially endemics, are particularly vulnerable to climate change [18]. Our findings support this expectation, as both future climatic scenarios indicate a drastic reduction in projected AOO, elevating the species' classification to Endangered (EN; AOO = 20.8 km²) according to IUCN Red List criterion A3(c) [60].

In this context, investigating the genetic diversity profile of *N. barbata* populations is essential to evaluate their resilience to climate change and the species' extinction risk based on its gene pool and the drivers of suitable area loss [79-80] Although the natural populations analyzed here remain within areas projected to be climatically suitable in the future, some occur at the edges of this suitability threshold (MU in Pernambuco state and SP in Paraíba), and all are located outside PA. This suggests that under extreme climatic conditions, habitat suitability for *N. barbata* will be severely restricted, increasing threats to the maintenance of genetic diversity in both haplogroups (N and S).

The divergence between the northern and southern populations of *Neesiochloa barbata* (~ 6 Ma) coincides with the global expansion of C4 grass-dominated biomes and the establishment of strong water seasonality regimes in South America [81-82]. The emergence of a seasonally arid climate during the late Miocene acted as a key selective driver in the Caatinga domain and Neotropical SDTF in South America [1,83]. In this scenario, the acquisition or fixation of an annual life history in *N. barbata* can be interpreted as an evolutionary mechanism of drought avoidance [84], which accelerates generation time, restricts gene flow due to phenological mismatch, and acts as a promoter of the observed genetic structuring and vicariance. Notably, the *N. barbata* accession sequence (GenBank, GU359634.1; *Swallen 4491* US) corresponds to a sample from Ceará state (CE). Although limited by Sanger sequencing compared to our novel genomic dataset, and given that our sampling lacks populations from CE, this accession offers a distinct perspective on the divergence timing, suggesting that populations belonging to this lineage may be older in CE (~ 12 Ma).

In the future, nearly half (43.6%) of all favorable areas for this species will be within PA. Although there is an increase in the proportion of protected habitat (from 39% to 43%) in the most pessimistic scenario, the total suitable area is shrinking much faster than the suitable area within PA. It is crucial to critically reflect on this scenario apparent increase in protection. This result demonstrates that current PA will serve as future climatic refugia, concentrating protected remnants in areas that remain climatically stable (Figure S2), rather than reflecting the creation of new PA [33]. Furthermore, the awns on *N. barbata* diaspores promote long-distance dispersal [85-86]. This capacity likely drives gene flow among populations and may

explain the high diversity observed in the plastome (cpDNA). Therefore, to mitigate species extinction, conservation strategies must combine the refugial role of PAs with the natural potential of *N. barbata* to reach new environmentally suitable areas.

We recommend that the protected area system in the Caatinga SDTF be expanded to a territorial extent to connect already threatened habitats as a policy to strengthen natural protected areas. Although Caatinga conservation is closely associated with combating desertification [59], climate change is expected to cause increasingly severe droughts throughout Northeast Brazil [87-88]. This scenario highlights the functional importance of PA in the Caatinga as *in situ* conservation measures for the genetic heritage of endemic groups that are particularly sensitive to climate dynamics in SDTF [88-89]. A similar case was reported for *Penstemon coriaceus* W. Schaffn. ex A. Gray (Plantaginaceae), whose genetically isolated populations require a conservation network integrating both *in situ* and *ex situ* strategies to ensure genetic diversity under climate change [80].

The highest climatic suitability indices for *Neesiochloa barbata* will be concentrated in the northernmost portion of the Caatinga. This geographic pattern underscores the importance of strengthening PA in this region, particularly as predictors of future priority conservation efforts for grasses in the Brazilian semi-arid region [33]. Furthermore, future suitability projections reinforce the relevance of protecting key populations such as MU (which acts as a bridge between northern and southern genetic groups) and CA, which harbors a private allele (CA06).

The marked differentiation of genetic clusters, especially revealed by population structure data and haplotype networks, indicates that populations are structured both genetically and geographically in cpDNA. Consequently, conserving only one of the two haplogroups (N or S) would be insufficient to maintain the overall genetic diversity of the species. Similar patterns have been reported for species of *Zea* L. (Poaceae: Panicoideae) [90], where the diversity of native maize (teosintes) is strongly structured at local scales. Effective conservation strategies for *N. barbata* should prioritize the protection of the localities where populations occur, with special attention to peripheral populations (MU and SP) in areas that will remain stable in the future.

Beyond climatic variables, areas with low suitability values (purple spots; Fig. 3) may reflect a synergistic effect of anthropogenic disturbances (both chronic and acute) widely documented in the Caatinga [7]. Our results suggest that projections from the most pessimistic scenario (SSP5–8.5) are already detectable in current reality: historically recorded populations (especially in the state of Bahia) were not relocated during our field expeditions. Notably, these localities already coincide with areas the model identifies as having low future suitability (threshold < 60%). This suggests that climate dynamics and habitat degradation may be shaping the distribution of *N. barbata* at an accelerated pace, suggesting that impacts predicted for the end of the century may already be emerging under current climatic conditions.

The Caatinga is one of Brazil's most threatened phytogeographic domains [13] Substantial efforts have been made to map and identify areas of high conservation priority and biological importance [33]. Expanding protected area coverage in the Caatinga is likely the

primary tool for conserving native flora, although this debate is not new [91] and has led to limited practical advances in environmental policies for this vegetation type in Brazil [92]. Approximately half of the original vegetation cover has already been lost, and current knowledge of the rich endemic biodiversity of the Caatinga [8,13] reinforces the need to critically evaluate whether the existing protection network will be capable of conserving a representative fraction of this diversity in the future. Therefore, assessing disturbances such as climate change impacts on the distribution of flagship species like *N. barbata* must be a central component of pragmatic environmental policies aiming to conserve the genetic heritage of the endemic flora of the Caatinga SDTF.

Therefore, conservation policymakers must integrate spatial projections with genomic data to design resilient conservation networks under the climate crisis [93-94]. Protecting intra-specific diversity determines whether species maintain their adaptive potential [95] which demands that decision-makers expand protected areas (PA) to encompass the full gene pool as key populations of *N. barbata* demonstrate (MU acting as a bridge between haplogroups, and CA harboring a private allele). To complement *in situ* measures, conservation programs should prioritize the collection and long-term storage of *N. barbata* in seed germplasm banks [96]. Investigating seed germination biology and propagation mechanisms will ground our phylogeographic and climate suitability findings to build effective area restoration strategies, ultimately preserving the evolutionary potential and genetic heritage of the endemic Caatinga flora [80].

Acknowledgements

We thank the funding agencies involved in the logistical and financial support provided throughout this study: Conselho Nacional de Desenvolvimento Científico e Tecnológico (CNPq; grant numbers: 140208/2023-2, 315433/2023-0, 404718/2024-8), Fundação de Amparo à Pesquisa do Estado de Minas Gerais (FAPEMIG; grant numbers: APQ-03015-24, APQ-05111-25); and ProEx/PPGBV Resources, (CAPES Financial Code 001), with special thanks to the Mohamed bin Zayed Species Conservation Fund (MBZ; grant number: 230533323). We extend our gratitude to Dr. Fátima Araújo, MSc. Emanoel Messias, Izabel Paiva, Everton Amorim, Kaiane Varjão, BS. José Vinícius, and the staff of the Seridó Ecological Station (ESEC-Seridó SisBio license number: 93931) for their assistance during fieldwork and the search for new populations. Finally, we thank MSc. Taciane Schröder, Dr. Paulo Aecyo and, Dr. Gustavo Souza for their insightful comments that improved this manuscript.

Fund

Mohamed bin Zayed Species Conservation Fund (MBZfund), FAPEMIG, CAPES, CNPq

Conflict of Interest Statement

The authors declare that they have no competing financial, personal, or professional interests that could have influenced the work reported in this paper.

Data Availability Statement

All genomic datasets, including population genetic diversity indices, AMOVA outputs, DAPC clustering analysis files, and haplotype network source data supporting the findings of this

study, have been deposited in the Zenodo Repository (https://doi.org/10.5281/zenodo.23223015). Nucleotide sequences (nrDNA cistron and plastid genome markers) are supported in the NCBI GenBank database under accession numbers indicated in Table-S2, and information generated from this study is available in GenBank BioProject under accession number PRJNA1542439 (https://www.ncbi.nlm.nih.gov/sra/PRJNA1542439). Custom scripts and distribution datasets are available from the corresponding author upon reasonable request.

Ethics Statements

The authors declare that this study was conducted in accordance with Wiley's Best Practice Guidelines on Publishing Ethics and Research Integrity. All plant samples were collected outside Protected Areas; therefore, specific collection permits from regulatory agencies (ICMBio/IBAMA) were not required. Nevertheless, field sampling of botanical material in the Caatinga was conducted under SISBIO permit number 93931/1. All individuals who contributed to the study, from field data collection to statistical analysis and data interpretation, regardless of their academic degree, were given the opportunity to participate in discussing and drafting the manuscript and are included as co-authors.

Author contributions

YC - Conceptualization, Methodology, Formal analysis, Resources, Writing - Review & Editing;

JN - Formal analysis, Writing - Review & Editing;

APH – Conceptualization, Methodology, Resources, Writing - Review & Editing;

YLS - Formal analysis, Writing - Review & Editing;

JRM - Conceptualization, Methodology, Resources, Writing - Review & Editing;

CADW - Conceptualization, Methodology, Resources, Writing - Review & Editing, Supervision;

MA - Conceptualization, Methodology, Resources, Writing - Review & Editing, Supervision.

Supplementary table - S1. Contribution of the bioclimatic variables, with mean, median, and standard deviation across all scenarios. More information's available in WorldClim.org.

Supplementary table - S2. Genbank accession numbers for nrDNA (ITS) and cpDNA (*rps16-trnK*, *rps16* intron, *rpl32-trnL, ndhF*, and *ndhA* intron) sequences and herbarium vouchers for the Pappophorinae species included in the phylogenetic analyses.

Supplementary figure – S1. Visual characterization of the landscapes of some visited areas based on records of the previously known geographic distribution of *Neesiochloa barbata.* The map contrasts historical occurrence records (red circles) with the current field expeditions (stars: visited areas and populations found; and squares: visited areas and populations not found). **(A)** Shrub–herbaceous Caatinga landscape surrounding the population found in Salgueiro, PE. **(B)** Landscape surrounding the population found in Timbaúba dos Batistas, RN. **(C)** Stony–sandy soil vegetated by specimens of *N. barbata*. **(D)** Open Caatinga landscape surrounding the population found in Salgueiro, PE. **(E)** Aspect of the area visited in

Itatim, BA, consisting of anthropized Caatinga, with no population found. **(F)** Aspect of the area visited in Morro do Chapéu, BA, with no population found. **(G)** Landscape aspects of the area of a previously recorded population in Jaguarari, BA (*Melo 6192*, HUEFS 148176), where no populations were found.

Supplementary figure – S2. Projected shifts in environmental suitability for *Neesiochloa barbata* within the Caatinga SDTF by the end of the century (2080–2100). Maps represent consensus dynamics comparing current conditions against two climate scenarios: **(A)** SSP2-4.5 (optmistic scenario) and **(B)** SSP5-8.5 (pessimistic scenario). Areas are classified into suitability gain (blue), stability (grey), and loss (red). Light grey lines delimit protected areas for conservation (PA), the solid black line marks the Caatinga SDTF border, and blue dots indicate the genetically analyzed populations.

Supplementary figure - S3. FastTree maximum-likelihood phylogenetic tree of *Neesiochloa barbata* and allied Pappophorinae taxa derived from plastid DNA (cpDNA). Node values represent Shimodaira–Hasegawa-like (SH-like) local support calculated in FastTree v2.1.11. This topology provides statistical node support for the time-calibrated phylogeny presented in Figure 6.

Supplementary figure - S4. Bayesian phylogenetic tree of *Neesiochloa barbata* based on nrDNA (ITS). The topology displays a widespread lack of internal resolution, characterized by extensive polytomies and low or null node support. *Sporobolus maritimus* serves as the outgroup. Node values indicate posterior probabilities.

Supplementary figure - S5. FastTree maximum-likelihood phylogenetic tree of *Neesiochloa barbata* based on nrDNA (ITS). Southern populations (MU, PF) and two northern individuals (TB02, TB05) collapse into a basal polytomy. The remaining northern samples (CA, SP, TB01, TB03, TB04) form a sister lineage, with CA06 as the most basal branch. *Sporobolus maritimus* serves as the outgroup. Node value indicates local support.

References

[1] Pennington, R. T., Prado, D. E. & Pendry, C. A. (2000). Neotropical seasonally dry forests and Quaternary vegetation changes. *Journal of Biogeography*, 27(2), 261–273. https://doi.org/10.1046/j.1365-2699.2000.00397.x

[2] Malhi, Y., Gardner T.A., Goldsmith G.R., Silman M.R. & Zelazowski P. (2014) Tropical forests in the Anthropocene. *Annual Review of Environment and Resources*, 39, 125–159.

[3] Miles, L., Newton A.C., DeFries R.S., Ravilious C., May I., Blyth S., *et al.* (2006) A global overview of the conservation status of tropical dry forests. *Journal of Biogeography*, 33, 491–505.

[4] Antonelli A. (2022). The rise and fall of Neotropical biodiversity. *Botanical Journal of the Linnean Society*, 199, 8–24. https://doi.org/10.1093/botlinnean/boab061

631 [5] O'Neill, B. C. & Oppenheimer, M. (2004). Climate change impacts are sensitive to the
632 concentration stabilization path. *Proceedings of the National Academy of Sciences*, *101*(47),
633 16411-16416. doi.org/10.1073/pnas.0405522101

634 [6] Smith, S. J., Edmonds, J., Hartin, C. A., Mundra, A. & Calvin, K. (2015). Near-term
635 acceleration in the rate of temperature change. *Nature Climate Change*, *5*(4), 333-336.
636 https://doi.org/10.1038/nclimate2552

637 [7] Silva, J. M. C., Leal, I. R. & Tabarelli, M. (Eds.). (2018). Caatinga: the largest tropical dry
638 forest region in South America. Springer.

639 [8] Fernandes, M.F., Cardoso D. & Queiroz L.P. (2020) An updated plant checklist of the
640 Brazilian Caatinga seasonally dry forests and woodlands reveals high species richness and
641 endemism. *Journal of Arid Environments*, 174, 104079.

642 [9] Marengo, J. A. & Bernasconi, M. (2015). Regional differences in aridity/drought conditions
643 over Northeast Brazil: present state and future projections. *Climatic Change*, *129*(1), 103-
644 115. doi 10.1007/s10584-014-1310-1

645 [10] Ribeiro, E.M.S., Arroyo-Rodríguez, V., Santos, B.A., Tabarelli, M. & Leal, I.R. (2015),
646 Chronic anthropogenic disturbance drives the biological impoverishment of the Brazilian
647 Caatinga vegetation. J Appl Ecol, 52: 611-620. https://doi.org/10.1111/1365-2664.12420

648 [11] Marengo, J.A., Torres R.R. & Alves L.M. (2017) Drought in Northeast Brazil—past,
649 present, and future. *Theoretical and Applied Climatology*, 129, 1189–1200.

650 [12] Souza, B. I. D., Artigas, R. C. & Lima, E. R. V. D. (2015). Caatinga e desertificação.
651 *Mercator (Fortaleza)*, *14*(1), 131-150. doi 10.4215/RM2015.1401. 0009

652 [13] Moro M.F., Amorim V.O., Queiroz L.P. de, Costa L.R.F. da, Maia R.P., Taylor N.P. &
653 Zappi D.C. (2024) Biogeographical districts of the Caatinga dominion: a proposal based on
654 geomorphology and endemism. *The Botanical Review*, 90, 1–54.

655 [14] Andrade-Lima D. (2007) Estudos fitogeográficos de Pernambuco. *Anais da Academia*
656 *Pernambucana de Ciência Agronômica*, 4, 243–274.

657 [15] Luebert F. (2021) The two South American dry diagonals. *Frontiers of Biogeography*, 13,
658 e52052.

659 [16] BFG – The Brazil Flora Group. (2022) Leveraging the power of a collaborative scientific
660 network. *Taxon*, 71, 178–198. https://doi.org/10.1002/tax.12640

661 [17] FFB - Flora e Funga do Brasil. (2026). Jardim Botânico do Rio de Janeiro. Available at:
662 http://floradobrasil.jbrj.gov.br/ (Accessed August 2026)

663 [18] Silva, J. L. S. E., Cruz-Neto, O., Peres, C. A., Tabarelli, M. & Lopes, A. V. (2019). Climate
664 change will reduce suitable Caatinga dry forest habitat for endemic plants with
665 disproportionate impacts on specialized reproductive strategies. *PloS one*, *14*(5), e0217028.

666 [19] Loarie S.R., Carter B.E., Hayhoe K., McMahon S., Moe R., Knight C.A. & Ackerly D.D.
667 (2008) Climate change and the future of California's endemic flora. *PLoS ONE*, 3, e2502.

668 [20] Foden W.B., Young B.E., Akçakaya H.R., Garcia R.A., Hoffmann A.A., Stein B.A., *et al.*
669 (2019) Climate change vulnerability assessment of species. *Wiley Interdisciplinary*
670 *Reviews: Climate Change*, 10, https://doi.org/10.1002/wcc.551.

671 [21] Elith, J. & Leathwick J.R. (2009) Species distribution models: ecological explanation and
672 prediction across space and time. *Annual Review of Ecology, Evolution, and Systematics*,
673 40, 677–697. https://doi.org/10.1146/annurev.ecolsys.110308.120159

674 [22] Peterson A.T., Papeş M. & Eaton M. (2011). Transferability and model evaluation in
675 ecological niche modeling: a comparison of GARP and Maxent. *Ecography*, 34, 550–560.
676 https://doi.org/10.1111/j.1600-0587.2010.06305.x

677 [23] Vieilledent G., Cornu C., Sanchez A.C., Pock-Tsy J.M.L. & Danthu P. (2013)
678 Vulnerability of baobab species to climate change and effectiveness of the protected area
679 network in Madagascar. *Biological Conservation*, 166, 11–22.

680 [24] Jeschke J.M. & Strayer D.L. (2008) Usefulness of bioclimatic models for studying climate
681 change and invasive species. *Annals of the New York Academy of Sciences*, 1134, 1–24.

682 [25] Sosa, V., Loera, I., Angulo, D. F., Vásquez-Cruz, M. & Gándara, E. (2019). Climate
683 change and conservation in a warm North American desert: Effect in shrubby plants. *PeerJ*,
684 *7*, doi e6572.

685 [26] Hosseini, N., Mehrabian, A. & Mostafavi, H. (2021). Modeling climate change effects on
686 spatial distribution of wild *Aegilops* L. (Poaceae) toward food security management and
687 biodiversity conservation in Iran. *Integrated Environmental Assessment and Management*,
688 *18*(3), 697-708.

[27] Davoudnia B., Dadkhodaie A., Naderi R., van Slageren M., Pourkhorshid Z. & Ekhlasi M. (2024) Diversity and eco-geographical distribution pattern of some *Aegilops* species from the Zagros and Alborz mountain ranges of Iran. *Plant Ecology*, 235, 1–14.

[28] Lou, R. N., Jacobs, A., Wilder, A. P. & Therkildsen, N. O. (2021). A beginner's guide to low-coverage whole genome sequencing for population genomics. *Molecular Ecology*, *30*(23), 5966-5993. doi 10.1111/mec.16077

[29] Hohenlohe, P. A., Funk, W. C. & Rajora, O. P. (2021). Population genomics for wildlife conservation and management. *Molecular ecology*, *30*(1), 62-82.

[30] Yu J., Hu S., Wang J., Wong G.K.S., Li S., Liu B., *et al.* (2002) A draft sequence of the rice genome (*Oryza sativa* L. ssp. *indica*). *Science*, 296, 79–92. https://doi.org/10.1126/science.1068037

[31] Schnable, P. S., Ware, D., Fulton, R. S., Stein, J. C., Wei, F., Pasternak, S., et al. (2009). The B73 maize genome: complexity, diversity, and dynamics. *Science*, *326*(5956), 1112-1115. doi 10.1126/science.1178534

[32] Redford, K. (Ed.), Brooks, T. (Ed.), Macfarlane, N. (Ed.), Adams, J. (Ed.), Alphey, L., Bennet, E., Delborne, J., Eggermont, H., Esvelt, K., Kingirl, A., Kokotovich, A., Kolodziejczyk, B., Kuiken, T., Mead, A., Oliva, M., Perello, E., Slobodian, L., Thizy, D., Tompkins, D. et al. (2019). *Genetic frontiers for conservation: An assessment of synthetic biology and biodiversity conservation*. IUCN. https://doi.org/10.2305/IUCN.CH.2019.05.en

[33] MMA (2018) *2ª Atualização das Áreas Prioritárias para Conservação, Utilização Sustentável e Repartição dos Benefícios da Biodiversidade Brasileira*. Ministério do Meio Ambiente, Secretaria de Biodiversidade, Brasília, DF. Available from: https://www.gov.br/mma/pt-br/assuntos/biodiversidade-e-biomas/biomas-e-ecossistemas/conservacao-1/areas-prioritarias/2a-atualizacao-das-areas-prioritarias-para-conservacao-da-biodiversidade-2018 [Accessed 24 August 2025].

[34] Luikart, G., England, P.R., Tallmon, D., Jordan, S. & Taberlet, P. (2003). The power and promise of population genomics: from genotyping to genome typing. *Nature reviews genetics*, *4*(12), 981-994. https://doi.org/10.1038/nrg1226

718 [35] Coates, D. J., Byrne, M. & Moritz, C. (2018). Genetic diversity and conservation units:
719 dealing with the species-population continuum in the age of genomics. *Frontiers in ecology*
720 *and evolution*, *6*, 165. https://doi.org/10.3389/fevo.2018.00165

721 [36] Oliveira, R.P. & Valls, J.F.M. 2024. *Neesiochloa barbata* (Nees) Pilg. *in* Flora e Funga
722 do Brasil. Jardim Botânico do Rio de Janeiro. Available at:
723 https://floradobrasil.jbrj.gov.br/FB20417 (Accessed 24 Aug 2025).

724 [37] Clayton W.D., Vorontsova M.S., Harman K.T. & Williamson H. (2006 onwards)
725 *GrassBase – the online world grass flora*. Royal Botanic Gardens, Kew.
726 www.kew.org/data/grasses-db.html

727 [38] IUCN. (2024). *The IUCN Red List of Threatened Species*. Version 2024-1.
728 https://www.iucnredlist.org (accessed 15 August 2024).

729 [39] Index Herbariorum (2026, continuously updated). Index Herbariorum: A Global Directory
730 of Public Herbaria and Associated Staff. New York Botanical Garden. Published online:
731 https://sweetgum.nybg.org/science/ih/ (accessed august 2026).

732 [40] GBIF (2026). GBIF Occurrence Download. Global Biodiversity Information Facility.
733 Available at: https://www.gbif.org (accessed: 15 August 2026).

734 [41] Reflora. (2026). Reflora – Herbário Virtual. Jardim Botânico do Rio de Janeiro. Available
735 at: https://reflora.jbrj.gov.br (Accessed: 15 August 2026).

736 [42] SpeciesLink. (2026). speciesLink Network. Instituto Nacional de Ciência e Tecnologia
737 em Modelos Ecológicos e Conservação. Available at: https://specieslink.net (Accessed: 15
738 August 2026).

739 [43] Fick S.E. & Hijmans R.J. (2017) WorldClim 2: new 1-km spatial resolution climate
740 surfaces for global land areas. *International Journal of Climatology*, 37, 4302–4315.

741 [44] Booth T.H., Nix H.A., Busby J.R. & Hutchinson M.F. (2014) BIOCLIM: the first species
742 distribution modelling package, its early applications and relevance to most current MaxEnt
743 studies. *Diversity and Distributions*, 20, 1–9.

744 [45] R Core Team, R. (2024, January). *R: A language and environment for statistical*
745 *computing*.

[46] Sánchez-Tapia, A., Mortara, S.R., Bezerra Rocha, D.S., Mendes Barros, F.S., Gall, G. & de Siqueira, M.F. (2020). modleR: a modular workflow to perform ecological niche modeling in R. *BioRxiv*, 2020-04.

[47] Phillips, S. J., Anderson, R. P., Dudík, M., Schapire, R. E. & Blair, M. E. (2017). Opening the black box: An open-source release of Maxent. *Ecography*, 40(7), 887-893.

[48] Guisan, A., Edwards Jr, T. C. & Hastie, T. (2002). Generalized linear and generalized additive models in studies of species distributions: setting the scene. Ecological modelling, 157(2-3), 89-100.

[49] Karatzoglou, A., Smola, A., Hornik, K. & Zeileis, A. (2004). kernlab-an S4 package for kernel methods in R. *Journal of statistical software*, 11, 1-20.

[50] Meyer, D., Dimitriadou, E., Hornik, K., Weingessel, A., Leisch, F., Chang, C. C. & Lin, C. C. (2019). e1071: misc functions of the department of statistics, probability theory group (formerly: E1071), TU Wien. R package version, 1(2).

[51] Liaw, A. & Wiener, M. (2002). Classification and regression by randomForest. *R news*, 2(3), 18-22.

[52] Hijmans, R. J., Phillips, S., Leathwick, J. & Elith, J. (2017). dismo: Species distribution modeling. R package version, 1(4), 1-1.

[53] Allouche O., Tsoar A. & Kadmon R. (2006). Assessing the accuracy of species distribution models: prevalence, kappa and the true skill statistic (TSS). *Journal of Applied Ecology*, 43(6), 1223–1232. https://doi.org/10.1111/j.1365-2664.2006.01214.x

[54] Liu C., White M. & Newell G. (2013). Selecting thresholds of occurrence in the prediction of species distributions. *Ecography*, 36(10), 1141–1153. https://doi.org/10.1111/j.1600-0587.2013.00120.x

[55] Hijmans R.J. (2023) *raster: geographic data analysis and modeling*. R package version 3.6-20.

[56] Gutierrez, E.E. & Heming, N.M. (2018). Introducing AIC model averaging in ecological niche modeling: a single-algorithm multi-model strategy to account for uncertainty in suitability predictions. *arXiv preprint arXiv:1807.04346*.

774 [57] Heming, N.M., Dambros, C. & Gutierrez, E.E. (2019). Advanced Techniques for
775 Ecological Niche Modeling Made Easy (R package version: 0.4.2.). Github:
776 https://github.com/HemingNM/ENMwizard

777 [58] UNEP-WCMC & IUCN. (2025). The World Database on Protected Areas (WDPA) [On-
778 line]. Cambridge, UK: UNEP-WCMC and IUCN. Available at:
779 https://www.protectedplanet.net (Accessed August 2025)

780 [59] MMA (2019) *Política Nacional de Combate à Desertificação e Mitigação dos Efeitos da*
781 *Seca*. Ministério do Meio Ambiente, Brasília, DF. Available from:
782 https://www.gov.br/participamaisbrasil/plano-de-acao-brasileiro-de-combate-a-
783 desertificacao-e-mitigacao-dos-efeitos-da-seca-pab-brasil-2024 [Accessed 24 August
784 2025].

785 [60] IUCN (2003) *Guidelines for Application of IUCN Red List Criteria at Regional and*
786 *National Levels: Version 3.0*. IUCN Species Survival Commission, IUCN, Gland,
787 Switzerland and Cambridge, UK.

788 [61] Pomoim, N., Hughes A.C., Trisurat Y. & Corlett R.T. (2022). Vulnerability to climate
789 change of species in pro tected areas in Thailand. *Scientific Reports* 12(1): 5705. doi:
790 10.1038/s41598-022-09767-9

791 [62] Lombo-Sanchez Y.J., Suarez-Contento K.Y., Pereira Silva M.P. & Pôrto K.C. (2025).
792 Liverworts in a changing world: vulnerability and extinction risk of specialist species under
793 climate change in a tropical country (Colombia). *Nature Conservation Research* 10(3): 34–
794 53. https://dx.doi.org/10.24189/ncr.2025.016

795 [63] Ferreira, M.E. & Grattapaglia, D. (1995). Introdução ao uso de marcadores moleculares
796 em análise genética. 2nd edn. Brasília: EMBRAPA-CENARGEN.

797 [64] Katoh, K. & Toh, H. (2008). Recent developments in the MAFFT multiple sequence
798 alignment program. *Briefings in Bioinformatics*, v. 9, n. 4, p. 286-298, 2008.
799 doi:10.1093/bib/bbn01

800 [65] Mäder, G., Zamberlan, P.M., Segatto, A.L.A., Stehmann, J.R., Bonatto, S.L. & Freitas,
801 L.B. (2021). When phylogeography meets niche suitability to unravel the evolutionary
802 history of a shrub from the Brazilian Atlantic Forest. *Botanical Journal of the Linnean*
803 *Society,* v. 195, n. 1, p. 77-92. https://doi.org/10.1093/botlinnean/boaa073

804 [66] Bandelt, H.J., Forster, P. & Röhl, A. (1999). Median-joining networks for inferring
805 intraspecific phylogenies. *Molecular Biology and Evolution*, v. 16, n. 1, p. 37-48,.
806 doi10.1093/oxfordjournals.molbev.a026036

807 [67] Leigh, J. W. & Bryant, D. (2015). POPART: full-feature software for haplotype network
808 construction. *Methods in Ecology & Evolution*, *6*(9), 1110.

809 [68] Excoffier, L., Smouse, P. E. & Quattro, J. M. (1992). Analysis of molecular variance
810 inferred from metric distances among DNA haplotypes: application to human mitochondrial
811 DNA restriction data. *Genetics*, *131*(2), 479-491.

812 [69] Excoffier, L., Laval, G. & Schneider, S. (2005). An integrated software package for
813 population genetics data analysis. *Evolutionary bioinformatics online*, *1*(4), 47-50. [Manual
814 Arlequin ver 3.5. http://cmpg.unibe.ch/software/arlequin3]

815 [70] Jombart, T. (2008). adegenet: a R package for the multivariate analysis of genetic markers.
816 *Bioinformatics*, 24(11), 1403-1405.

817 [71] Drummond, A. J., Suchard, M. A., Xie, D. & Rambaut, A. (2012). Bayesian phylogenetics
818 with BEAUti and the BEAST 1.7. *Molecular Biology and Evolution*, 29(8), 1969-1973.

819 [72] Yule, G.U. (1925). A mathematical theory of evolution, based on the conclusions of Dr.
820 J. C. Willis, F.R.S. *Philosophical Transactions of the Royal Society of London.* Series B,
821 Containing Papers of a Biological Character, 213, 21-87. doi10.1098/rstb.2023.0297

822 [73] Gernhard, T. (2008). The conditioned reconstructed process. J*ournal of Theoretical
823 Biology,* 253(4), 769-778. doi10.1016/j.jtbi.2008.04.005

824 [74] Rambaut, A., Drummond, A. J., Xie, D., Baele, G. & Suchard, M. A. (2018). Posterior
825 summarization in Bayesian phylogenetics using Tracer 1.7. *Systematic biology*, *67*(5), 901-
826 904.

827 [75] Price, M. N., Dehal, P. S. & Arkin, A. P. (2010). FastTree 2 – approximately maximum-
828 likelihood trees for large alignments. *PLoS ONE*, 5(3), e9490.
829 https://doi.org/10.1371/journal.pone.0009490

830 [76] Gallaher, T.J., Peterson, P.M., Soreng, R.J., Zuloaga, F.O., Li, D.Z., Clark, L.G. et al.
831 (2022). Grasses through space and time: An overview of the biogeographical and
832 macroevolutionary history of Poaceae. *Journal of Systematics and Evolution*, *60*(3), 522-
833 569. doi10.1111/jse.12857

[77] Olsen, J. T., Caudle, K. L., Johnson, L. C., Baer, S. G. & Maricle, B. R. (2013). Environmental and genetic variation in leaf anatomy among populations of *Andropogon gerardii* (Poaceae) along a precipitation gradient. *American Journal of Botany*, 100(10), 1957-1968.

[78] IUCN (2022) *Guidelines for Using the IUCN Red List Categories and Criteria. Version 15.1*. Prepared by the Standards and Petitions Committee. Available from: https://www.iucnredlist.org/resources/redlistguidelines [Accessed 24 August 2026].

[79] Wouw, M. V. D., Dijk, P. V. & Huiskes, A. H. (2008). Regional genetic diversity patterns in Antarctic hairgrass (*Deschampsia antarctica* Desv.). *Journal of Biogeography*, *35*(2), 365-376.

[80] Zacarías-Correa A.G., Lira-Noriega A., Pérez-Calix E., *et al.* (2020) Back to the future of a rare plant species of the Chihuahuan Desert: tracing distribution patterns across time and genetic diversity as a basis for conservation actions. *Biodiversity and Conservation*, 29, 1821–1840. https://doi.org/10.1007/s10531-020-01962-2

[81] Osborne, C. P. & Beerling, D. J. (2005). Nature's green revolution: the remarkable evolutionary rise of C4 plants. *Philosophical Transactions of the Royal Society B: Biological Sciences*, 361(1465), 173. doi: 10.1098/rstb.2005.1737.

[82] Edwards, E. J., Osborne, C. P., Strömberg, C. A., Smith, S. A., C4 Grasses Consortium, Bond, W. J. et al. (2010). The origins of C4 grasslands: integrating evolutionary and ecosystem science. *Science*, 328(5978), 587-591.

[83] Queiroz, L. P., Cardoso, D., Fernandes, M. F. & Moro, M. F. (2017). Diversity and evolution of flowering plants of the Caatinga domain. In Caatinga: The largest tropical dry forest region in South America (pp. 23-63). Cham: Springer International Publishing.

[84] Friedman, J. & Rubin, M. J. (2015). All in good time: understanding annual and perennial strategies in plants. *American Journal of Botany*, 102(4), 497.

[85] Petersen, K.B. & Kellogg, E.A. (2022). Diverse ecological functions and the convergent evolution of grass awns. *American journal of botany*, *109*(9), 1331-1345. https://doi.org/10.1002/ajb2.16060

[86] Couceiro, Y.D.S.V., Maciel, J.R., Costa, L., Kellogg, E.A., Welker, C.A.D., Peterson, P.M., & Alves, M. (2026). The Role of Awns Evolution in Shaping the Biogeographical

History of Pappophorinae (Poaceae: Chloridoideae). *Journal of Biogeography*, *53*(3). https://doi.org/10.1111/jbi.70201

[87] Salazar, L. F., Nobre, C. A. & Oyama, M. D. (2007). Climate change consequences on the biome distribution in tropical South America. *Geophysical Research Letters*, *34*(9), L09708, doi:10.1029/2007GL029695.

[88] Oliveira, G., Araújo M.B., Rangel T.F., Alagador D. & Diniz-Filho J.A.F. (2012) Conserving the Brazilian semiarid (Caatinga) biome under climate change. *Biodiversity and Conservation*, 21, 2913–2926.

[89] Santos, M.G., Oliveira, M.T., Figueiredo, K.V. *et al.* (2014). Caatinga, the Brazilian dry tropical forest: can it tolerate climate changes?. *Theoretical and Experimental Plant Physiology* 26, 83–99. https://doi.org/10.1007/s40626-014-0008-0

[90] Rivera-Rodríguez, D. M., Mastretta-Yanes, A., Wegier, A., De la Cruz Larios, L., Santacruz-Ruvalcaba, F., Ruiz Corral, J. A. et al. (2023). Genomic diversity and population structure of teosinte (Zea spp.) and its conservation implications. *Plos one*, *18*(10), e0291944.

[91] CBD (2010) *Strategic Plan for Biodiversity 2011–2020 and the Aichi Targets*. Secretariat of the Convention on Biological Diversity, Nagoya. Available from: https://www.cbd.int/sp [Accessed 24 August 2025]

[92] MMA (2015) *Fifth National Report to the Convention on Biological Diversity: Brazil*. Ministério do Meio Ambiente, Secretaria de Biodiversidade e Florestas, Brasília, DF. Available from: https://www.cbd.int/doc/world/br/br-nr-05-en.pdf [Accessed 24 August 2025].

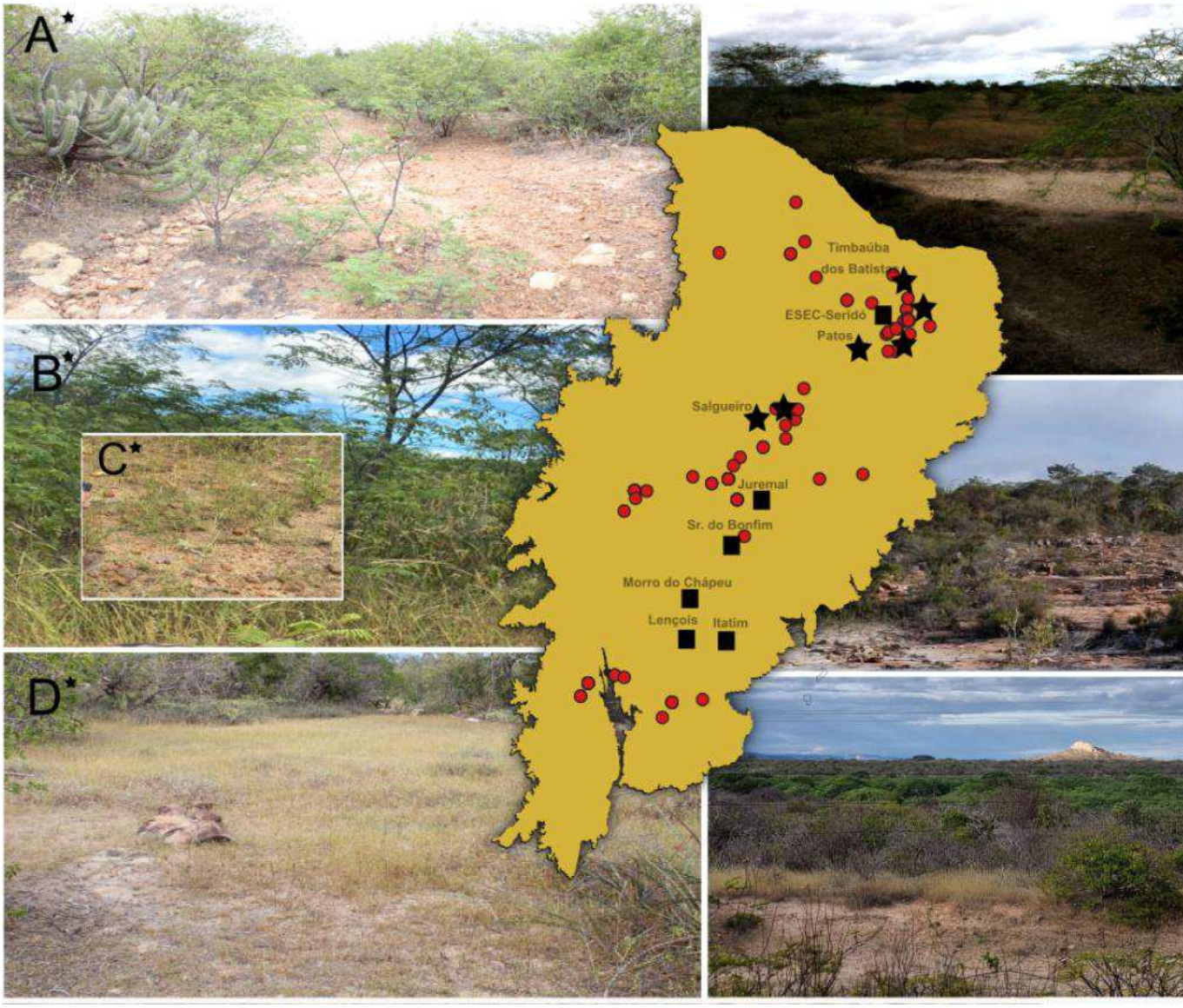
[93] Moritz, C. (2002). Strategies to protect biological diversity and the evolutionary processes that sustain it. *Systematic Biology*, 51(2), 238–254.

[94] Allendorf, F. W., Hohenlohe, P. A. & Luikart, G. (2010). Genomics and the future of conservation genetics. *Nature reviews genetics*, *11*(10), 697-709.

[95] Frankham, R., Ballou, J. D., Briscoe, D. A. & McInness, K. H. (2002). *Introduction to conservation genetics* (Vol. 617). Cambridge, UK: Cambridge university press.

892 [96] Li, D. Z. & Pritchard, H. W. (2009). The science and economics of ex situ plant
893 conservation. *Trends in Plant Science*, 14(11), 614–621.
894 https://doi.org/10.1016/j.tplants.2009.09.005

895 **Supplementary figure - S1**

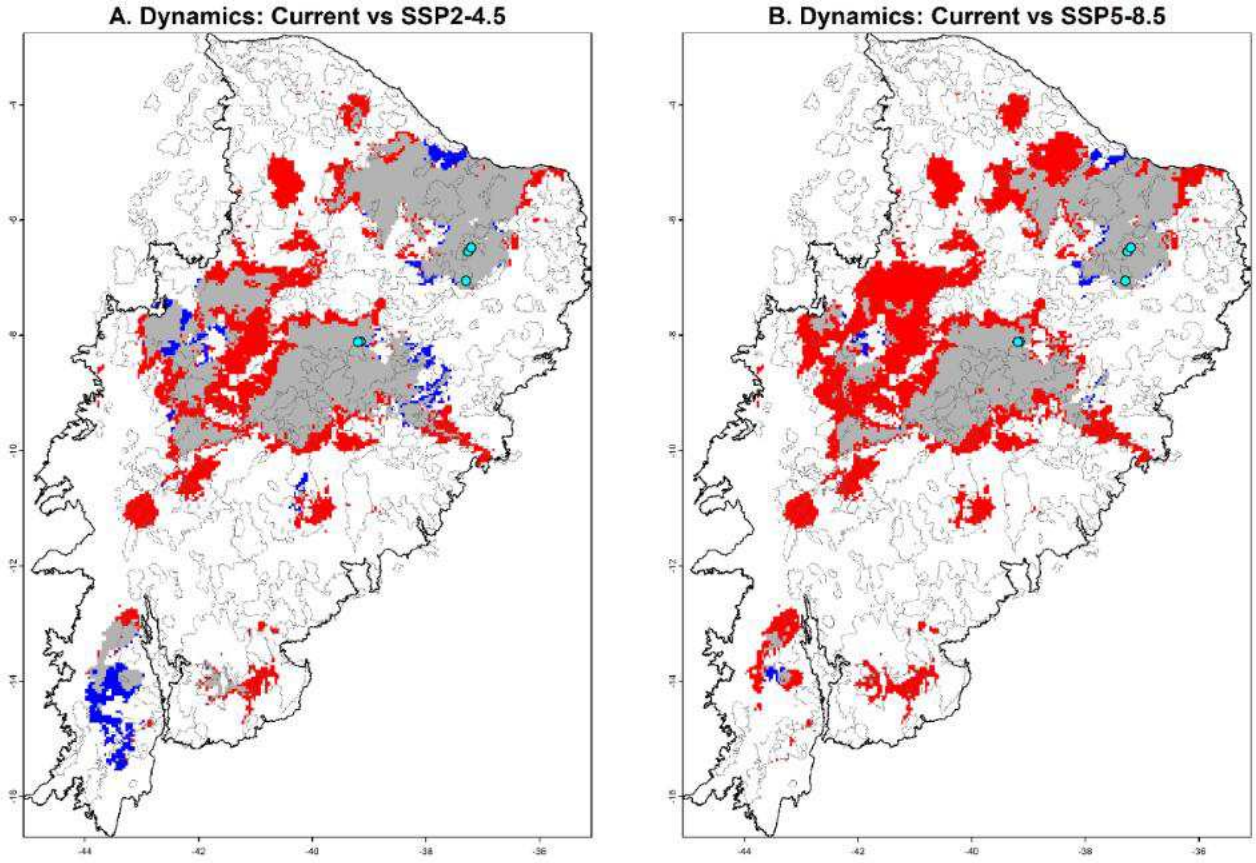


896

897

898

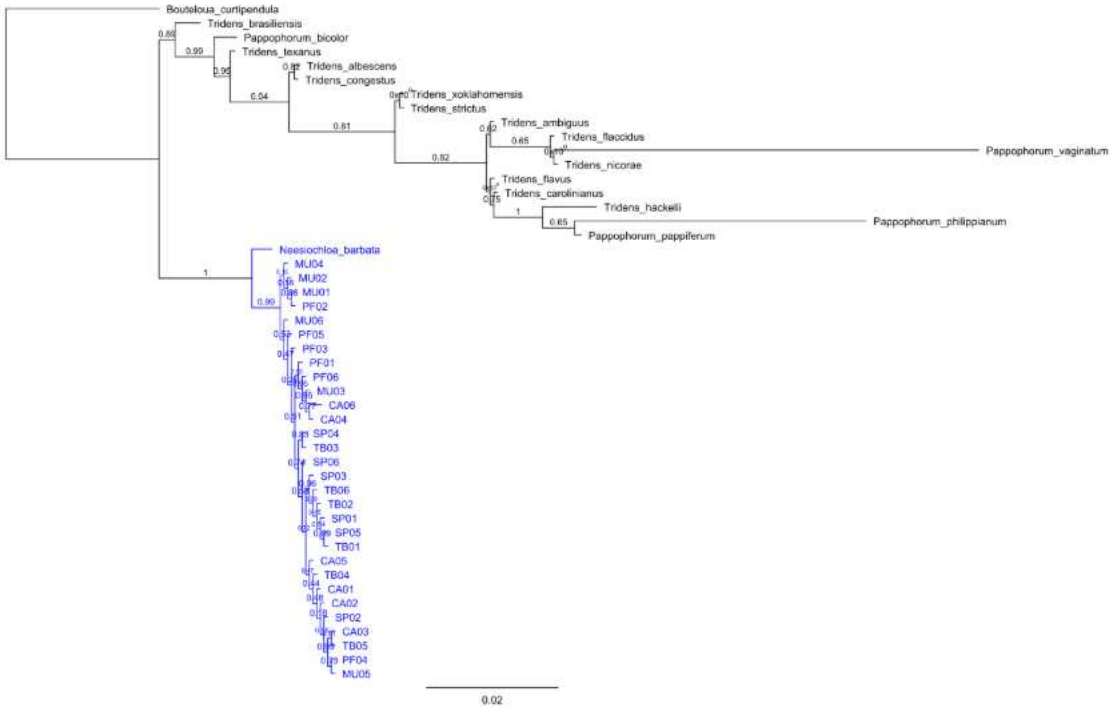
899 **Supplementary figure – S2**



900

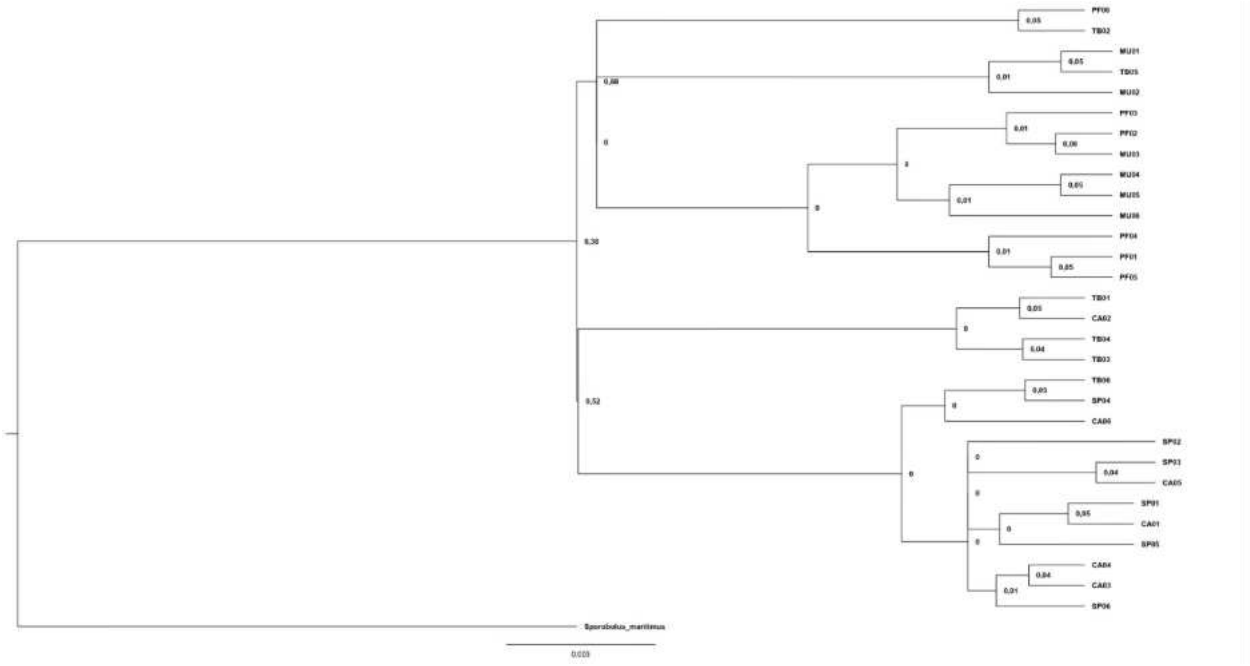
901

902 **Supplementary figure – S3**

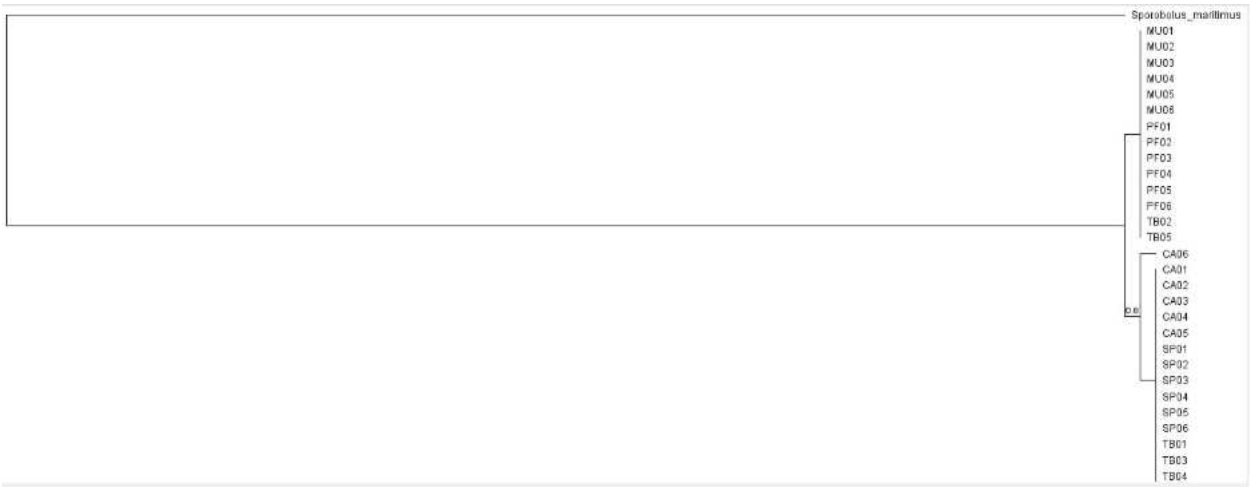


903

Supplementary figure –S4



Supplementary figure –S5



915

916

917

Supplementary table - S1.

Scenario	Climatic variable	Mean	Median	Standard deviation
Current	bio_3	73.44272	73.4282	3.752911
Current	bio_12	747.9615	754	173.89553
Current	bio_14	5.575092	2	7.537481
Current	bio_18	171.3791	170	72.725253
Current	bio_19	89.08974	57	109.277549
SSP2-4.5	bio_3	69.55867	68.8	4.405505
SSP2-4.5	bio_12	833.2766	829	184.930918
SSP2-4.5	bio_14	5.241758	2	6.792152
SSP2-4.5	bio_18	148.6984	145	86.062077
SSP2-4.5	bio_19	103.6636	53	145.064226
SSP5-8.5	bio_3	69.44377	68.6	5.327716
SSP5-8.5	bio_12	806.4469	787	209.967306
SSP5-8.5	bio_14	5.06044	2	6.385621
SSP5-8.5	bio_18	136.6328	131.5	85.410325
SSP5-8.5	bio_19	140.0562	52	186.648623

929 **Supplementary table - S2.**

species	ITS	*rps16-trnK*	*rps16 intron*	*rpl32-trnL*	*ndhF*	*ndhA intron*	voucher
Neesiochloa barbata	GU359122	GU360724	GU360279	GU360005	GU359634	–	Swallen 4491 (US)
Pappophorum bicolor	KX582397	KX582985	KX582914	KX582671	KX582557	KX582480	Pohl 12464 (MO)
Pappophorum pappiferum	GU359128	GU360700	GU360276	GU359996	GU359596	GU359402	Peterson 21689 (US)
Pappophorum philippianum	KJ768885	KX582986	KX582915	KJ768980	KX582558	KX582481	Renvoize 4225 (MO)
Pappophorum vaginatum	KX582399	KX582987	KX582916	KX582676	KX582561	–	Wagner 3930 (MO)
Tridens × oklahomensis	KX582416	–	–	KX582697	–	–	Barrell 138-73 (US)
Tridens albescens	KX582417	KX582995	KX582920	–	–	–	Reeder 4586 (US)
Tridens ambiguus	KX582418	KX582996	KX582922	KX582698	–	KX582484	Grelen 195 (US)
Tridens brasiliensis	KX582420	–	–	KX582699	–	–	Quarin 3794 (US)
Tridens carolinianus	KX582422	KX582998	KX582924	KX582702	–	KX582486	Boyce 1567 (US)
Tridens congestus	KX582423	KX582999	KX582925	KX582703	–	–	Trouart 35 (US)
Tridens flavus	KF827567	KF827816	KF827750	KF827688	KX582575	KF827614	Davidse 38002 (MO)
Tridens flavus var. chapmanii	KF827568	KF827817	KF827751	KF827689	KX582576	KF827615	McCanley 438 (MO)
Tridens hackelii	KX582431	–	–	KX582711	–	–	Rosengurtt 4544 (US)
Tridens nicorae	KX582434	KX583006	–	KX582715	–	–	Anderson 2428 (US)
Tridens strictus	KX582436	KX583008	KX582934	KX582716	KX582580	KX582488	Summers 9414 (MO)
Tridens texanus	KX582439	KX583009	KX582936	KX582719	–	KX582489	Reeder 4564 (US)

930

Supplementary Files

This is a list of supplementary files associated with this preprint. Click to download.

- graphicBICclustersrDNA.pdf
- summarycrossvalidationplastomeK2.csv
- graphicBICclustersplastomeK2.pdf
- haplotypedatafileplastomeannotatedmain.htm
- resultsBICplastomeK2.csv
- resultsBICrDNAK2.csv
- DAPCScatterPlastomak21.pdf
- summarycrossvalidationK2rDNA.csv
- haplotypedatafilerDNAannotatedmain.htm
- graphiccrossvalidationPCsrDNAK2.pdf
- DAPCScatterrDNAK2.pdf
- graphiccrossvalidationPCsK2plastoma.pdf
- moleculardiversityindicesplastome.xml